Article

Cell Chemical Biology

A *Pseudomonas aeruginosa* PQS quorum-sensing system inhibitor with anti-staphylococcal activity sensitizes polymicrobial biofilms to tobramycin

Graphical abstract

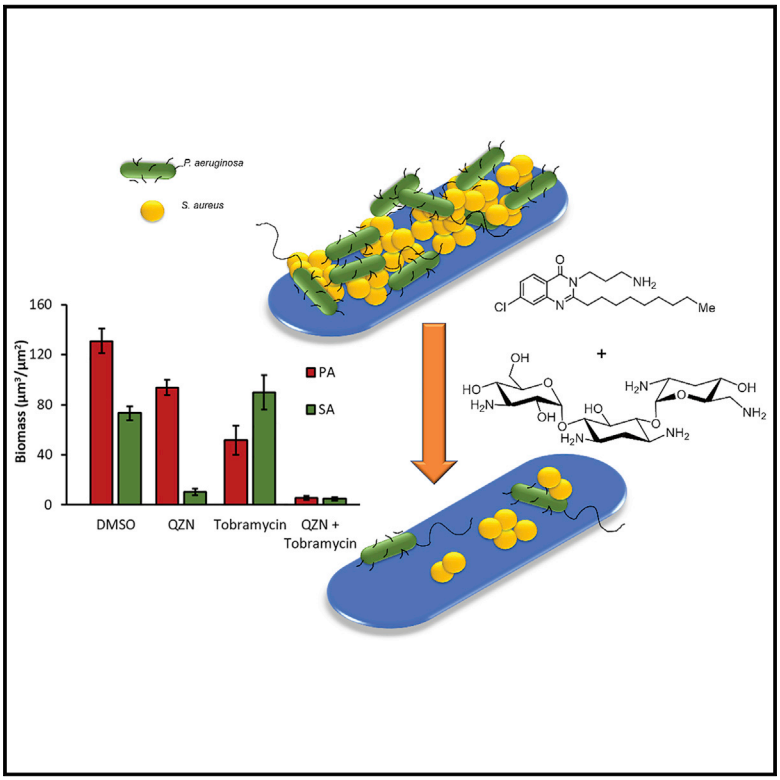

Authors

Ewan J. Murray, Jean-Frédéric Dubern, Weng C. Chan, Siri Ram Chhabra, Paul Williams

Correspondence

paul.williams@nottingham.ac.uk

In brief

P. aeruginosa and *S. aureus* cause biofilm-associated infections. Murray et al. demonstrate that quinazolinone inhibitors of *P. aeruginosa* quorum-sensing can be chemically modified to kill *S. aureus* biofilms and prevent *P. aeruginosa*-mediated protection of *S. aureus* against tobramycin. Tobramycin plus quinazolinone eradicates mixed *P. aeruginosa* and *S. aureus* biofilms.

Highlights

- QZNs inhibit PQS-dependent quorum sensing and reduce biofilm formation in *Pseudomonas aeruginosa*
- A subset of QZNs is bactericidal for planktonic *Staphylococcus aureus* and severely damages biofilms
- In mixed species biofilms, *P. aeruginosa* protects *S. aureus* from tobramycin
- Tobramycin plus QZN eradicates mixed *P. aeruginosa* and *S. aureus* biofilms

Murray et al., 2022, Cell Chemical Biology *29*, 1187–1199
July 21, 2022
https://doi.org/10.1016/j.chembiol.2022.02.007

CellPress

Cell Chemical Biology

CellPress
OPEN ACCESS

Article

A *Pseudomonas aeruginosa* PQS quorum-sensing system inhibitor with anti-staphylococcal activity sensitizes polymicrobial biofilms to tobramycin

Ewan J. Murray,[1,3] Jean-Frédéric Dubern,[1,3] Weng C. Chan,[2] Siri Ram Chhabra,[1] and Paul Williams[1,4,*]
[1]National Biofilms Innovation Centre, Biodiscovery Institute and School of Life Sciences, University of Nottingham, University Park, Nottingham NG7 2RD, UK
[2]School of Pharmacy, Biodiscovery Institute, University of Nottingham, University Park, Nottingham NG7 2RD, UK
[3]These authors contributed equally
[4]Lead contact
*Correspondence: paul.williams@nottingham.ac.uk
https://doi.org/10.1016/j.chembiol.2022.02.007

SUMMARY

As single- and mixed-species biofilms, *Staphylococcus aureus* and *Pseudomonas aeruginosa* cause difficult-to-eradicate chronic infections. In *P. aeruginosa*, pseudomonas quinolone (PQS)-dependent quorum sensing regulates virulence and biofilm development that can be attenuated via antagonists targeting the transcriptional regulator PqsR (MvfR). Here, we exploited a quinazolinone (QZN) library including PqsR agonists and antagonists for their activity against *S. aureus* alone, when co-cultured with *P. aeruginosa*, and in combination with the aminoglycoside tobramycin. The PqsR inhibitor, QZN 34 killed planktonic Gram-positives but not Gram-negatives. QZN 34 prevented *S. aureus* biofilm formation, severely damaged established *S. aureus* biofilms, and perturbed *P. aeruginosa* biofilm development. Although *P. aeruginosa* protected *S. aureus* from tobramycin in mixed biofilms, the combination of aminoglycoside antibiotic with QZN 34 eradicated the mixed-species biofilm. The mechanism of action of QZN 34 toward Gram-positive bacteria is shown to involve membrane perturbation and dissipation of transmembrane potential.

INTRODUCTION

Pseudomonas aeruginosa and *Staphylococcus aureus* are opportunistic human pathogens that are major causes of hospital- and community-acquired infections (Peleg and Hooper, 2010; Tong et al., 2015). They are members of the ESKAPE group of multi- and pan-antibiotic-resistant bacteria that cause acute and chronic infections in skin, blood, bone, and soft tissues as well as in the respiratory and urinary tracts (Peleg and Hooper, 2010; Tong et al., 2015; De Oliveira et al., 2020). They are also associated with difficult-to-eradicate biofilm-centered infections involving implanted medical devices and can be considered as shared ecological niche competitors, since they often co-exist at an infection site (Percival et al., 2015; Orazi and O'Toole, 2019). For example, non-healing diabetic foot ulcer infections, a serious complication of diabetes, are usually polymicrobial and biofilm-centered and often harbor both *P. aeruginosa* and *S. aureus* (Fazli et al., 2009; DeLeon et al., 2014). Similarly, their co-infection of the lungs of individuals with cystic fibrosis is indicative of poorer clinical outcomes than in those infected with either species alone (Orazi and O'Toole, 2019).

To facilitate co-existence within the same environmental niche, bacteria have evolved intricate regulatory networks that enable them to evade, counter, inhibit, or suppress other bacterial species and gain mutual benefit through increased biofilm production, high levels of tolerance to antimicrobial agents, and enhanced virulence (Hotterbeekx et al., 2017; Orazi and O'Toole, 2019). In this context and in contrast with the clinical situation (DeLeon et al., 2014), planktonic co-culture of *P. aeruginosa* with *S. aureus* usually results in the inhibition of staphylococcal growth and virulence factor production. This is mainly as a consequence of exposure to small-molecule exoproducts produced by *P. aeruginosa*, including phenazines, hydrogen cyanide, *N*-acylhomoserine lactones (AHLs), and 2-alkyl-4(1H)-quinolones (AQs) (Hotterbeekx et al., 2017; Orazi and O'Toole, 2019). In *P. aeruginosa* AHLs and AQs co-ordinately control secondary metabolite production, virulence gene expression and biofilm development through co-ordinated cell-cell communication or quorum sensing (QS) (Williams and Camara, 2009). However, *P. aeruginosa* QS signal molecules can also impact on other microbes including *S. aureus* sharing the same ecological niche. For example, *N*-(3-oxododecanoyl)-L-homoserine lactone and its base-catalyzed rearrangement product 5-hydroxyethyl-3-decanoyltetramic acid inhibit *S. aureus* growth (Kaufmann et al., 2005) and, at sub-inhibitory concentrations, virulence factor production through blockade of *agr*-dependent QS (Qazi et al., 2006; Murray et al., 2014).

P. aeruginosa also produces a diverse range of AQs and AQ *N*-oxides of various alkyl chain lengths and saturation states (Heeb

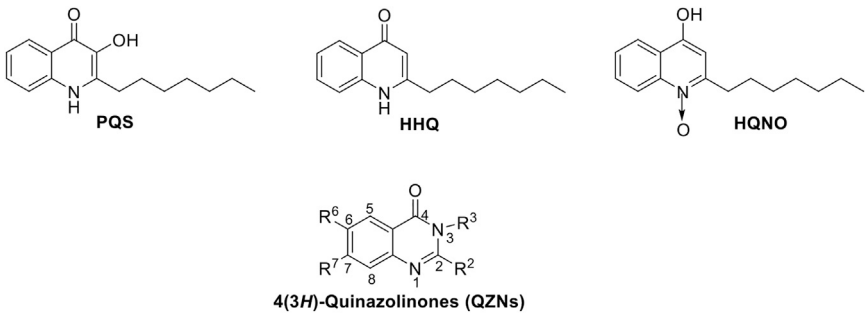

Figure 1. Structures of the AQs, PQS, HHQ, and HQNO and a generalized structure for the QZN series

et al., 2010). Apart from their role in AQ-dependent QS, AQs exhibit a range of biological activities from immune modulation and cytochrome inhibition to antimicrobial and iron-chelating activities (Hooi et al., 2004; Diggle et al., 2007; Nguyen and Oglesby-Sherrouse, 2016). For example, the AQ *N*-oxide 2-heptyl-4-hydroxyquinoline *N*-oxide (HQNO) (Figure 1) and the unsaturated analogue (*E*)-4-hydroxy-2-(non-1-en-1-yl)quinoline 1-oxide are effective inhibitors of *S. aureus* growth. Paradoxically, these *N*-oxides increase *S. aureus* persistence since, at sub-inhibitory concentrations and prolonged growth, they generate small-colony variants (SCVs) that show increased tolerance to aminoglycoside antibiotics (Orazi and O'Toole, 2019). When treated with HQNO, *S. aureus* biofilms become more sensitive to fluoroquinolones and membrane-targeting antibacterial agents but exhibit reduced susceptibility to vancomycin (Orazi and O'Toole, 2019; Orazi et al., 2019).

Given the global health threat posed by multi- and pan-antibiotic-resistant bacterial pathogens in single or polymicrobial infections, novel antibacterial agents are required that have unique modes of action and potent efficacy against biofilm-centered infections. In this context, the attenuation of bacterial virulence and biofilm formation have been viewed as attractive targets for the development of ''anti-virulence'' or ''anti-pathogenic'' agents that could be used individually or as antibiotic ''adjuvants'' in combination therapy (Williams, 2017). QS systems have therefore been considered promising targets for drug development (Rampioni et al., 2014; Williams, 2017).

In *P. aeruginosa*, AQ-dependent QS regulates virulence, biofilm development, and secondary metabolite production. *P. aeruginosa* mutants defective in AQ biosynthesis or perception are attenuated in experimental animal infection models (Déziel et al., 2005; Rampioni et al., 2010; Starkey et al., 2014; Dubern et al., 2015). Furthermore, the presence of AQs in sputum, blood, and urine correlates with clinical status cystic fibrosis patients suffering with chronic *P. aeruginosa* lung infections (Barr et al., 2015, 2017). Consequently, there has been considerable interest in AQ-dependent QS as a *P. aeruginosa* drug target and in particular the transcriptional regulator PqsR (also called MvfR) (Ilangovan et al., 2013; Starkey et al., 2014; Williams, 2017). 2-Heptyl-3-hydroxy-4(1*H*)-quinolone (PQS) and its biosynthetic precursor HHQ (2-heptyl-4-hydroxyquinoline) (Figure 1) function as the primary QS signal molecules in this system (Xiao et al., 2006; Heeb et al., 2010; Ilangovan et al., 2013). PQS and HHQ and their C9 congeners bind to and activate PqsR to trigger a positive feedback loop increasing expression of the *pqsABCDE* operon and, hence, AQ biosynthesis. PQS is also a ferric iron chelator and controls virulence, biofilm development, and the iron-starvation response via PqsR-dependent and PqsR-independent pathways (Diggle et al., 2007; Rampioni et al., 2016).

Potent inhibition of PqsR-mediated *pqsABCDE* expression and, hence, AQ biosynthesis has been achieved through ligand-based design, which has yielded PqsR antagonists ranging from quinolinones and quinazolinones (QZNs; Figure 1) to benzamide-benzimidazole and hydroxybenzamide derived molecules (Soukarieh et al., 2018). In addition to attenuating virulence, PqsR inhibitors have the added advantage of reducing the formation of antibiotic-tolerant persister cells (Starkey et al., 2014). From a series of (3*H*)-quinazolinones (3aza-AQs) screened as potential PqsR antagonists (Ilangovan et al., 2013), 12 QZN PqsR antagonists were identified, including 3-NH_2-7-Cl-C9-QZN (IC_{50} 5 μM; Table 1 compound **19**), which was shown to inhibit virulence factor production and biofilm development in *P. aeruginosa* (Ilangovan et al., 2013). Confirmation that **19** acted as a competitive PqsR antagonist was obtained by determination of the complex crystal structure of **19** bound within the PqsR ligand-binding domain. This revealed a similar orientation within the hydrophobic ligand-binding pocket as native AQ agonists (Ilangovan et al., 2013).

Given that **19** inhibits AQ-dependent QS in *P. aeruginosa* and that structurally related AQNOs display anti-staphyloccocal activity, we screened our library of 45 QZNs and related benzo [1,2,4]thiadiazines for activity against *S. aureus* and a range of other clinically relevant bacteria. Here, we present data that indicate that a subset of QZNs structurally related to **19**, and most notably 3-C_3NH_2-7Cl-C9-QZN **34** (PqsR IC_{50} 15 μM), kill planktonic Gram-positive pathogens including *S. aureus*, *Staphylococcus epidermidis*, *Streptococcus pyogenes*, and *Clostridioides difficile* but not Gram-negative bacteria such as *P. aeruginosa* and *Escherichia. coli*. Moreover, **34** inhibited *S. aureus* biofilm formation, damaged established *S. aureus* biofilms, and perturbed *P. aeruginosa* biofilm development. In mixed *S. aureus* and *P. aeruginosa* biofilms, **34** provided partial protection for *P. aeruginosa*. Although *P. aeruginosa* protected *S. aureus* from tobramycin in mixed biofilms, the combination of aminoglycoside and **34** eradicated the mixed-species biofilm. We also show that the mechanism of action of **34** involves binding and perturbation of the bacterial cytoplasmic membrane and disruption of transmembrane membrane potential.

RESULTS

Structure-activity relationship determination reveals the QZN structural features required for *S. aureus* growth inhibition

To evaluate the antibacterial activity of the QZN series, *S. aureus* strain RN6390B was first grown in the presence of 100 μM of each compound (Table 1). These included 43 QZNs and two

Table 1. QZN and BTD chemical structures and *S. aureus* growth-inhibitory properties

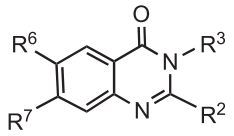

4(3*H*)-Quinazolinones (QZNs)

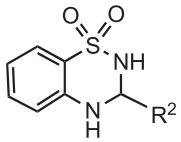

BTD

No.	R^2	R^3	R^6	R^7	Abbreviation	MIC (μM)
1	*n*-C_7H_{15}	H	H	H	C7-QZN	>100
2	*n*-C_9H_{19}	H	H	H	C9-QZN	>100
3	*n*-C_9H_{19}	H	H	F	7F-C9-QZN	>100
4	*n*-C_9H_{19}	H	H	Cl	7Cl-C9-QZN	>100
5	*n*-C_7H_{15}	H	H	H	C7-BTD	>100
6	*n*-C_9H_{19}	H	H	H	C9-BTD	>100
7	*n*-C_5H_{11}	NH_2	H	H	3-NH_2-C5-QZN	>100
8	*n*-C_7H_{15}	NH_2	H	H	3-NH_2-C7-QZN[a]	>100
9	*n*-C_9H_{19}	NH_2	H	H	3-NH_2-C9-QZN[a]	>100
10	*n*-$C_{11}H_{23}$	NH_2	H	H	3-NH_2-C11-QZN[a]	>100
11	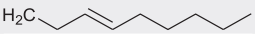	NH_2	H	H	3-NH_2-C9:3-QZN	>100
12	$Ph(CH_2)_3$	NH_2	H	H	3-NH_2-PhC3-QZN	>100
13	$Cy(CH_2)_3$	NH_2	H	H	3-NH_2-CyC3-QZN	>100
14	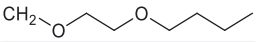	NH_2	H	H	3-NH_2-(2,5-dioxa-C9)-QZN	>100
15	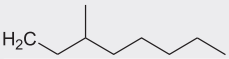	NH_2	H	H	3-NH_2-(3-Me-C8)-QZN	>100
16	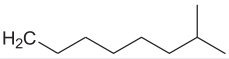	NH_2	H	H	3-NH_2-(7-Me-C8)-QZN	>100
17	*n*-C_1H_3	NH_2	H	H	3-NH_2-C1-QZN	>100
18	*n*-C_9H_{19}	NH_2	H	F	3-NH_2-7F-C9-QZN[a]	>100
19	*n*-C_9H_{19}	NH_2	H	Cl	3-NH_2-7Cl-C9-QZN[a]	>100
20	*n*-C_9H_{19}	NH_2	Cl	H	3-NH_2-6Cl-C9-QZN	>100
21	*n*-C_9H_{19}	NH_2	F	H	3-NH_2-6F-C9-QZN	>100
22	*n*-C_9H_{19}	NH_2	F	F	3-NH_2-6F,7F-C9-QZN[a]	>100
23	*n*-C_9H_{19}	NH_2	OMe	OMe	3-NH_2-6OMe,7OMe-C9-QZN	>100
24	*n*-C_9H_{19}	NH_2	H	CF_3	3-NH_2-7CF_3-C9-QZN	>100
25	$Ph(CH_2)_3$	NH_2	H	Cl	3-NH_2-7Cl-PhC3-QZN[a]	>100
26	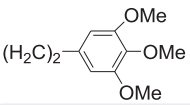	NH_2	H	Cl	3-NH_2-7Cl-(Tri-OMeC_6H_2)C2-QZN	>100
27	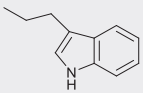	NH_2	H	Cl	3-NH_2-7Cl-(3-Ind) C2-QZN	>100
28	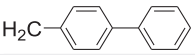	NH_2	H	Cl	3-NH_2-7Cl-BiPhC1-QZN	>100
29	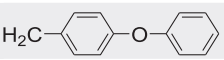	NH_2	H	Cl	3-NH_2-7Cl-PhOBn-QZN	>100
30	*n*-C_9H_{19}	$(CH_2)_2NH_2$	H	H	3-C_2NH_2-C9-QZN[a]	50
31	*n*-C_9H_{19}	$(CH_2)_2NH_2$	Cl	H	3-C_2NH_2-6Cl-C9-QZN[a]	25–50
32	*n*-C_9H_{19}	$(CH_2)_2NH_2$	H	Cl	3-C_2NH_2-7Cl-C9-QZN[a]	12.5
33	$Ph(CH_2)_3$	$(CH_2)_2NH_2$	H	Cl	3-C_2NH_2-7Cl-PhC3-QZN[a]	100
34	*n*-C_9H_{19}	$(CH_2)_3NH_2$	H	Cl	3-C_3NH_2-7Cl-C9-QZN[a]	6.25[c]

(*Continued on next page*)

Table 1. *Continued*

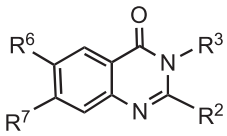

4(3*H*)-Quinazolinones (QZNs)

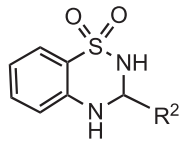

BTD

No.	R^2	R^3	R^6	R^7	Abbreviation	MIC (μM)
35	*n*-C_9H_{19}	$(CH_2)_4NH_2$	H	Cl	3-C_4NH_2-7Cl-C9-QZN	12.5
36	*n*-C_7H_{15}	OMe	H	H	3-OMe-C7-QZN	>100
37	*n*-C_9H_{19}	OMe	H	H	3-OMe-C9-QZN	>100
38	*n*-C_9H_{19}	OMe	H	Cl	3-OMe-7Cl-C9-QZN[b]	>100
39	*n*-C_9H_{19}	OMe	H	F	3-OMe-7F-C9-QZN[b]	>100
40	*n*-C_9H_{19}	OMe	F	F	3-OMe-6F,7F-C9-QZN[b]	>100
41	*n*-C_7H_{15}	NMe_2	H	H	3-NMe_2-C9-QZN	>100
42	*n*-C_9H_{19}	OH	H	H	3-OH-C9-QZN[b]	100
43	*n*-C_9H_{19}	OH	H	F	3-OH-7F-C9-QZN[b]	100
44	*n*-C_9H_{19}	OH	H	Cl	3-OH-7Cl-C9-QZN[b]	50
45	*n*-C_9H_{19}	CH_2OH	H	Cl	3-C_2OH-7Cl-C9-QZN	>100

[a]indicates known PqsR antagonist.
[b]indicates known PqsR agonist (Ilangovan et al., 2013).
[c]MIC increased to 25 μM in the presence of 10% FBS.

related benzo[1,2,4]thiadiazines (BTDs) that were synthesized (see Schemes 1 and 2 for examples) with mono-, di-, tri-, and tetra-ring substitutions. For each QZN that abolished growth, a minimum inhibitory concentration (MIC) was generated (Table 1). QZNs with varying 2-alkyl chains and especially with the 3-position unsubstituted (**1–4**) or substituted with NH_2 (**7–29**), OMe (**36–40**), NMe_2 (**41**), and CH_2OH (**45**) had MICs in excess of 100 μM. These results strongly suggest that endocyclic hydrazide and *O*-methyl hydroxamate functionalities would result in inactive analogs. Two related BTD derivatives (**5** and **6**) incorporating cyclic sulfonamide (-SO_2NH) (sultam) motif were also inactive. Compound **42** (3OH-C9-QZN), however, gave a MIC of 100 μM that improved with chlorine substitution at the 7-position (**44**). Growth-inhibitory activity improved markedly when the 3-position was substituted with an aminoalkyl [$(CH_2)_nNH_2$, where n = 2, 3, or 4] group (**30–35**)]. The MICs for this class of QZN suggested that, besides an aminoalkyl substituent at position-3, the presence of a 9-carbon alkyl chain at position-2 and a chlorine at position-7 were required for optimal activity. These systematic modifications resulted in the lead compounds **32** (3-C_2NH_2-7Cl-C9-QZN) and **34** (3-C_3NH_2-7Cl-C9-QZN), which gave the lowest MICs (12.5 μM [4.4 μg/mL] and 6.25 μM [2.3 μg/mL], respectively). We next sought to improve the potency of **34** by extending the aminoalkyl chain from C_3NH_2 to C_4NH_2 (**35**); however, this increased the MIC 2-fold to 12.5 μM.

Growth-inhibitory properties of 3-C_2NH_2-7Cl-C9-QZN 32 and 3-C_3NH_2-7Cl-C9-QZN 34

Compound **32** was assessed for the ability to inhibit the growth of clinically relevant bacterial pathogens. The MIC data shown in Table S1 demonstrate that **32** inhibits the growth of Gram-positives, including methicillin-sensitive *S. aureus* (MSSA) strains RN6390B and SH1000 and *S. aureus* hospital- (BH1CC) and community-acquired (USA300) methicillin-resistant *S. aureus* (MRSA) strains, as well as *S. epidermidis*, *Streptococcus pyogenes*, *Streptococcus agalactiae* and *C. difficile.* Nine recent MRSA isolates resistant to diverse conventional antibiotics were also tested and found to be similarly susceptible to **32**, with a MIC of 12.5 μM; **32** was, however, inactive as a growth inhibitor of the Gram negatives, *E. coli*, and *P. aeruginosa.* To determine whether the active QZNs were bacteriostatic or bactericidal, *S. aureus*, *S. epidermidis*, and *P. aeruginosa* were assessed in a bactericidal assay using a dose of 50 μM of **34** (8× MIC for *S. aureus*). Figure 2 shows that the number of viable planktonic *S. aureus* and *S. epidermidis* cells was reduced by three logs within 3 h, indicating that **34** is indeed bactericidal against both *S. aureus* and *S. epidermidis*, whereas the viable count for *P. aeruginosa* increased over the equivalent time frame.

Anti-staphylococcal biofilm properties of 3-C_3NH_2-7Cl-C9-QZN 34

The impact of **34** on biofilms formed by *S. aureus* USA300, the hospital-acquired MRSA strain BH1CC, as well as the laboratory prototype *S. aureus* and *S. epidermidis* strains SH1000 and 1457 was investigated. Biofilms were treated with **34** either immediately after cell attachment or once the biofilm had established (24 h post-attachment). Conversion of the redox-sensitive dye resazurin to the fluorescent product resorufin was used as an indicator of biofilm metabolic activity. Figure 3A indicates high fluorescence for all four staphylococcal biofilms exposed to the DMSO vehicle control, suggesting that a metabolically active biofilm had established after 24-h growth. Exposure to as little as 10 μM of **34** immediately after attachment (Figure 3A) resulted in a substantial loss of metabolic activity. Addition of **34** to a mature

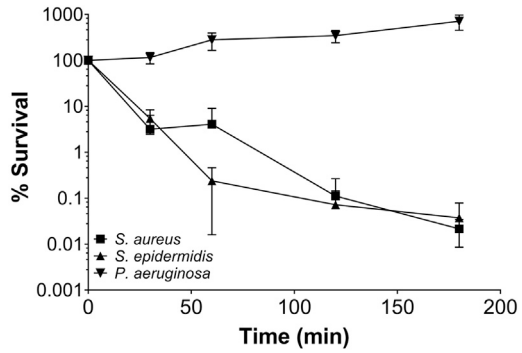

Figure 2. 3-C_3NH_2-7Cl-C9-QZN (QZN 34) is bactericidal for *S. aureus* and *S. epidermidis* but not for *P. aeruginosa*

Planktonic *S. aureus* USA300 JE2, *S. epidermidis* 1457 or *P. aeruginosa* PAO1 were treated with 50 μM (8× the *S. aureus* MIC) of compound **34**. The data presented are the mean viable counts (CFU) per mL from three independent experiments ±SD.

staphylococcal biofilm (Figure 3B), at a concentration of 50 μM (8× MIC), resulted in a 2-fold reduction in fluorescence compared with the vehicle control, whereas treatment with 100 μM **34** (16× MIC) reduced fluorescence to background for all four staphylococcal strains tested. Although resazurin provides useful information on biofilm viability, alternative methods are required to determine the impact of **34** on biofilm architecture. To further investigate our initial findings, biofilms were established over 24 h with *S. aureus* cells (SH1000) constitutively expressing green fluorescent protein (GFP) and counterstained with propidium iodide (PI) for live/dead quantification after challenge with increasing concentrations of **34** for 2 h. Confocal microscopy was used to generate the representative images shown in Figure 3C and quantified with respect to biofilm biomass and dead cells (Figure 3D). The data clearly show that *S. aureus* biofilms treated with the vehicle control had a biomass composed of cells expressing GFP with no visible red fluorescence (PI), indicative of viable, undamaged *S. aureus* cells and biofilms. Treatment with increasing concentrations of **34** revealed a concentration-dependent increase in red fluorescence (PI) and a reciprocal reduction in green fluorescence, confirming that the bacterial cells were either severely damaged or dead. In addition, viable count experiments demonstrated that whereas **34** completely inhibited biofilm formation, mature biofilms treated with **34** were more refractory, exhibiting an ~1.5 log reduction in viable counts (Figure S1). Taken together, the data shown in Figures 2, 3, and S1 show that **34** can damage and kill both planktonic and biofilm *S. aureus*.

3-C_3NH_2-7Cl-C9-QZN 34 perturbs *P. aeruginosa* biofilm development

Since PqsR inhibitors including **19** (3NH_2-7Cl-C9-QZN) inhibit *P. aeruginosa* biofilm development (Ilangovan et al., 2013), we examined the effect of **34**, which has an IC_{50} for PqsR of 15.5 μM Figure 4 shows the impact of **34** on *P. aeruginosa* biofilm formation. Biofilm biomass and extracellular DNA (eDNA) content were reduced by as little as 10 μM **34**, with a substantial reduction in biomass (~50%) clearly apparent at 100 μM **34** and with very little eDNA detectable (Figure 4).

S. aureus protects *P. aeruginosa* in a mixed-species biofilm from the effects of 3-C_3NH_2-7Cl-C9-QZN 34

Fluorescently labeled *S. aureus* (GFP, green) and *P. aeruginosa* (mCherry, red) were co-cultured to form mixed biofilm. Figure 5A shows that the biomass of the mixed biofilm is significantly greater (~5×) than that formed by each individual organism (compare Figures 3D and 4B with 5B). When incubated with **34** at 100 μM, GFP fluorescence is reduced by ~90%, suggesting that *S. aureus,* as with the single-species biofilm (Figure 3), succumbs to treatment with **34** (Figures 5A and 5B). However, despite a prolonged treatment time (4 h instead of 2 h) the red fluorescence of *P. aeruginosa* is only marginally reduced (~15%), suggesting that in the presence of *S. aureus P. aeruginosa* is protected to some extent from the effects of **34**.

3-C_3NH_2-7Cl-C9-QZN and tobramycin in combination are highly active against mixed biofilms

The aminoglycoside tobramycin is commonly used to treat chronic biofilm-associated *P. aeruginosa* infections in cystic fibrosis patients (Beaudoin et al., 2017). To determine whether 3-C_3NH_2-7Cl-C9-QZN **34** in combination with tobramycin could eradicate both *P. aeruginosa* and *S. aureus* in mixed biofilms, we first examined the susceptibility of *S. aureus* and *P. aeruginosa* monoculture biofilms to **34** in the presence and absence of tobramycin (Figure S2). For both pathogens, the combination of tobramycin and QZN was more effective than either compound alone. When we co-cultured with *P. aeruginosa* in the presence of tobramycin alone, we observed that the *S. aureus* biomass was protected, whereas the *P. aeruginosa* biomass was reduced by ~60% (Figures 5C and 5D). However, when **34** and tobramycin were used in combination, they reduced biofilm biomass by >95% for both bacterial species in the mixed biofilm (Figures 5C and 5D).

Cytotoxicity of 3-C_2NH_2-7Cl-C9-QZN 32 and 3-C_3NH_2-7Cl-C9-QZN 34 for eukaryotic cells

Since **34** showed excellent antibacterial activity, cytotoxicity for eukaryotic cells was assessed. Hemolysis assays (Figure S3A) indicated that **34** has an IC_{50} of 173 μM, which is ~28 times higher than the MIC (6.25 μM) for *S. aureus* and ~69 times the MIC generated for *C. difficile* (Table S1). Similar results were also observed with **32** (see Figure S3A). The non-growth-inhibitory *P. aeruginosa* PqsR-inhibitory QZN compound **19** was not hemolytic (Figure S3A). The release of lactate dehydrogenase from Jurkat cells after 24-h incubation with **34** is shown in Figure S3B. Data indicate that exposure to **34** resulted in an ~30% loss of cytoplasmic lactate dehydrogenase at concentrations above 6.3 μM; however, the total amount of lactate dehydrogenase released did not increase above 50% in the presence of up to 100 μM of **34**; therefore, an IC_{50} could not be generated. However, since the Jurkat cell assay medium includes 10% fetal bovine serum (FBS), we repeated the *S. aureus* MIC for **34** with FBS. This increased the MIC to 25 μM (Table 1), suggesting that the QZN binds to serum proteins, which would also reduce mammalian cytotoxicity. These data collectively suggest that **32** and **34** possess some limited selectivity for bacterial membranes.

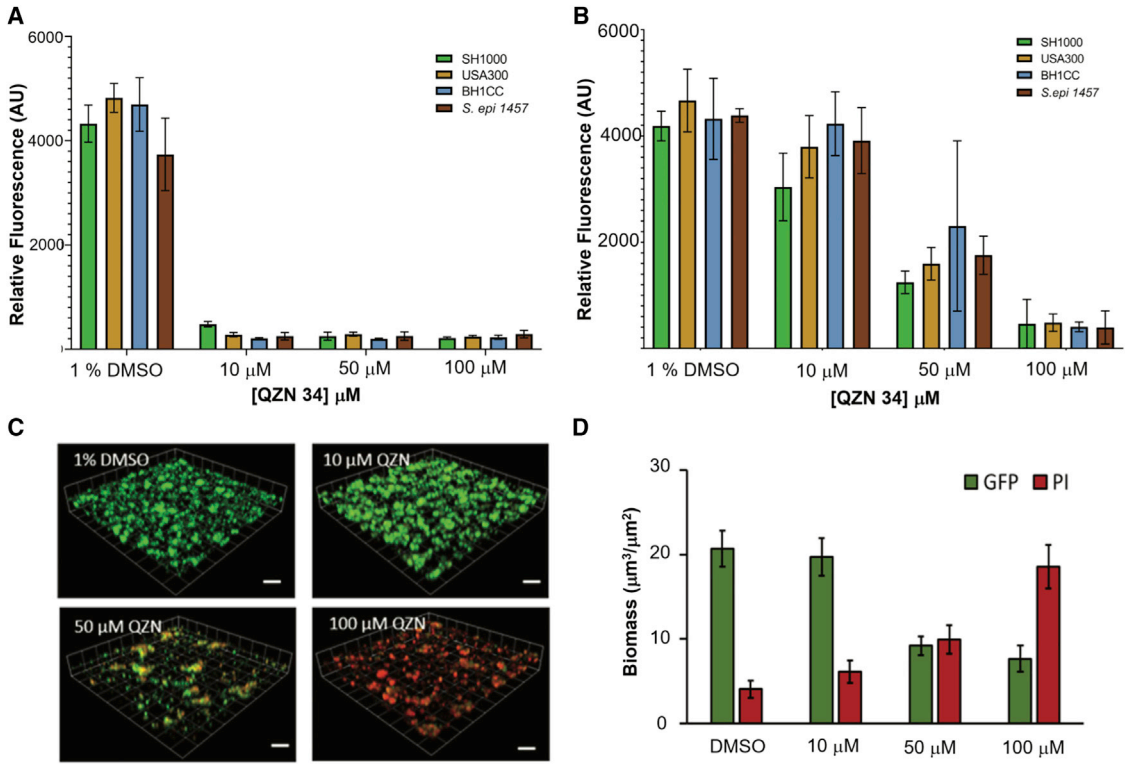

Figure 3. 3-C_3NH_2-7Cl-C9-QZN 34 inhibits staphylococcal biofilm formation

(A and B) Resazurin was used to assess the metabolic activity of *S. aureus* MRSA (USA300 and BH1CC), MSSA (SH1000) strains, and *S. epidermidis* staphylococcal biofilms treated with increasing concentrations of **34** directly after attachment (A) or after formation of mature biofilms (B). Data are means from 3 independent experiments ± SD.

(C) 3D confocal microscope images of mature GFP-labeled *S. aureus* biofilms treated with **34** for 4 h.

(D) Quantification of biofilm biomasses shown in (C). Dead cells and extracellular DNA (red) were stained with propidium iodide (PI; 2μM). Scale bars, 50 μm. Data are means from 3 independent experiments ± SD.

Mechanism of action of 3-C_2NH_2-7Cl-C9-QZN and 3-C_3NH_2-7Cl-C9-QZN for *S. aureus*

A potential explanation for QZN-mediated staphylococcal growth-inhibitory activities given the structural similarity to the AQs was reduced availability of ferric iron, since some AQs are ferric iron chelators. Although 3OH-C9-QZN **42** in common with PQS sequestered iron, neither **32** nor **34** possessed iron-chelating properties (Figure S4). The potency of **34** increased when the assay medium osmolality was reduced by replacing LB with sterile water. Under these conditions, **34** at 10 μM (~1.5× MIC for *S. aureus*) resulted in a rapid 2.5 log reduction in viable *S. aureus* cells after only 1 h of exposure (Figure S5). The provision of ionic solutes (NaCl, KCl, or $CaCl_2$) protected *S. aureus* from the bactericidal activity of **34**. These data suggested that 3-C_3NH_2-7Cl-C9-QZN **34** was likely to bind to and perturb the staphylococcal cell membrane.

Antibacterial agents that target the cytoplasmic membrane often disrupt essential electrical potentials, such as the transmembrane potential, that that are required to maintain essential cellular processes. Consequently, we first determined whether the QZNs interact with staphylococcal membranes, by utilizing the fluorescent dye di-8-ANEPPS, to monitor changes in dipole potential that permit quantification of membrane binding affinities and information on binding specificity (Murray et al., 2014). Figure 6A shows the changes in fluorescence ratio after the addition of a series QZNs based on their structures and SAR for *S. aureus* growth inhibition initially at a fixed concentration (40 μM). The PqsR agonist C9-PQS and closely related QZN, C9-QZN **2** had little impact on membrane dipole potential, which increased following the introduction of $3NH_2$, 3OH, and 7Cl substituents as for **9**, **19**, **42**, and **44**, although these compounds exhibited either no (**9**, **19**, and **42**) or very weak (**44**) growth-inhibitory activity. The greatest changes in dipole potential were noted for the growth-inhibitory QZNs **32**, **34**, and **35**. Subsequently, binding curves were constructed for selected QZNs by plotting changes in dipole potential against concentration (Figure 6B). These show that **32**, **34**, and **35** bound in a saturable-specific manner with similar high affinities (K_{ds} 22 ± 1.7, 6.6 ± 0.2, and 5.2 ± 0.3 μM, respectively) and that the data obtained fit a hyperbolic function consistent with a non-cooperative, single-site receptor-binding model (Figure 6B).

The bacterial membrane potential (ΔΨ) is a key component of the proton motive force (PMF) and is generated by selective ionic inclusion/expulsion. The cationic fluorescent dye Disc(3)5 can be used to assess the membrane-perturbing effects of the QZNs on ΔΨ. Figures 6C and S6 show that, after initial uptake and quenching of the fluorescent dye, addition of the growth-inhibitory QZNs **32** or **35** results in an increase in fluorescence as

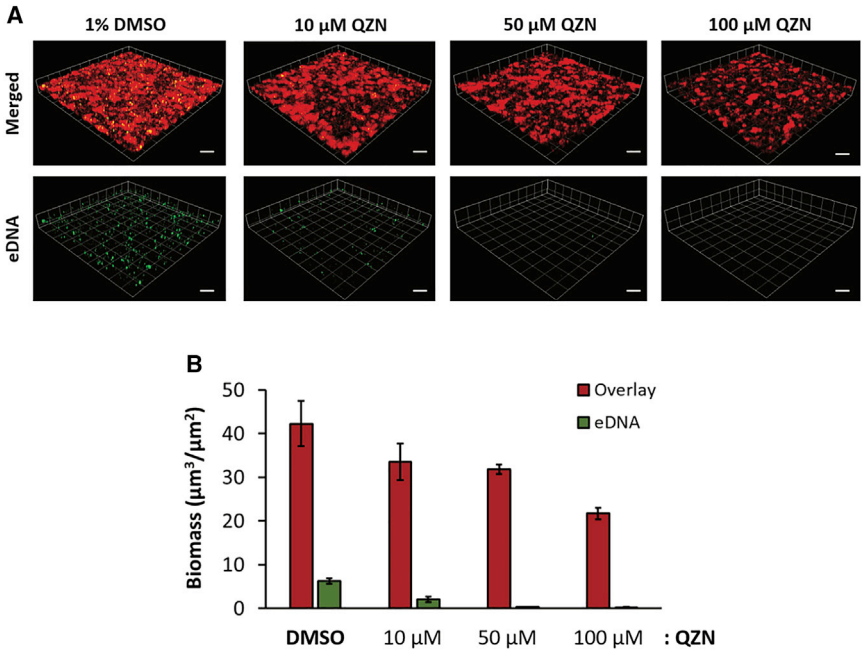

Figure 4. Effect of 3-C_3NH_2-7Cl-C9-QZN 34 on *P. aeruginosa* PAO1 biofilm formation

(A) 3D confocal microscope images showing mCherry-tagged *P. aeruginosa* biofilms grown in RPMI 1640 for 24 h in the presence of either DMSO (vehicle control) or QZN **34** (10, 50, and 100 μM). Scale bars, 50 μm.

(B) Biomass quantification of *P. aeruginosa* biofilms. Extracellular DNA was stained with Yoyo-1 (2 μM). Data are means from 3 independent experiments ± SD.

the cationic dye is released down a concentration gradient. In contrast, the non-growth-inhibitory QZN **19**, despite its ability to bind to the membrane, does not increase fluorescence (Figure S6A). Addition of the ionophore valinomycin as a positive control (Figures 6C and S6) but not antibiotics such as novobiocin and chloramphenicol (which do not target the cytoplasmic membrane) confirmed dye release as dependent on $\Delta\Psi$ depolarization. Although significant, the loss of $\Delta\Psi$ after addition of either **32** or **35** is unlikely to fully account for rapid cell death (Figure 2A). Consequently, the impact of the QZNs on membrane integrity was also investigated by evaluating uptake of the membrane-impermeable dye PI and the loss of ATP. The data presented in Figure 6D show that incubation with **32**, **34**, or **35**, but not **19** or **33**, resulted in significant cellular ATP loss alongside the reciprocal uptake of PI.

DISCUSSION

To discover compounds capable of attenuating biofilm formation and rendering biofilms more susceptible to conventional antibiotics for *S. aureus* individually and in co-culture with *P. aeruginosa*, we screened our library of QZNs for staphylococcal growth inhibition. Whereas 36 out of 45 compounds screened had MICs >100 μM, 3-OH-7Cl-C9-QZN **44** had a MIC of 50 μM for *S. aureus*. However, for *P. aeruginosa*, this compound is a PqsR agonist (Ilangovan et al., 2013) and therefore likely to enhance rather than inhibit *P. aeruginosa* virulence and biofilm formation. Replacement of the 3-hydroxy with 3-amino converted 3-OH-7Cl-C9-QZN **44** from a PqsR agonist to a potent antagonist (3-NH_2-7Cl-C9-QZN **19**) (Ilangovan et al., 2013). Although the amino substitution at the 3-position failed to improve the MIC for *S. aureus*, anti-staphylococcal activity was markedly enhanced by an aminoalkyl group (**30–32**; **34**, **35**), with **34** being the most potent compound (MIC 6.25 μM; 2.3 μg/mL). The MICs for this class of QZN suggested that, besides an aminoalkyl substituent at position-3, the presence of a 9-carbon alkyl chain at position-2 and a chlorine at position-7 were required for optimal activity. Whereas these compounds are PqsR antagonists with **30** being the most potent (IC_{50} 9.3 μM), compounds **32** and **34** were more active toward staphylococci and other Gram-positive pathogens while retaining good PqsR-inhibitory activity (IC_{50}s 19.3 and 15.5 μM, respectively; Ilangovan et al., 2013). These compounds were therefore selected for further evaluation. Although bactericidal for *S. aureus*, **32** and **34** do not inhibit *P. aeruginosa* planktonic growth. However, PQS-dependent QS regulates the release of eDNA, which is an important component of the *P. aeruginosa* biofilm extracellular matrix and is involved in the attachment, aggregation, and stabilization of microcolonies during *P. aeruginosa* biofilm formation (Allesen-Holm et al., 2006). eDNA also contributes to the tolerance of biofilms toward antibiotics such as tobramycin (Chiang et al., 2013; Wilton et al., 2015). 3-C_3NH_2-7Cl-C9-QZN **34** substantially inhibited *P. aeruginosa* biofilm formation and reduced eDNA to almost undetectable levels, consistent with its activity as a PqsR inhibitor.

Apart from its bactericidal activity against planktonic *S. aureus* strains as well as *S. epidermidis*, **34** substantially inhibited the metabolic activity of staphylococcal biofilms at concentrations as low 10 μM, while at 100 μM it effectively damaged mature biofilms. In mixed biofilms with *P. aeruginosa*, **34** eradicated *S. aureus*, although in this context it showed reduced efficacy against *P. aeruginosa*. Interspecies interactions have long been known to impact on the sensitivity profiles of bacteria to antimicrobial agents within multispecies biofilms via different mechanisms (Orazi and O'Toole, 2019). However, here, it is unclear whether the increased resistance of *P. aeruginosa* is simply due to the much greater biomass of the mixed- compared with the single-species biofilms so reducing the dose of **34** or whether it is a consequence of sequestration into staphylococcal membranes, given the mode of action of the QZN. Alternatively, the presence of *S. aureus* within the biofilm may alter the physiology of *P. aeruginosa*, resulting in a more QZN-resistant phenotype. In this context, cell aggregation caused by the binding of *S. aureus* protein A adhesin to the *P. aeruginosa* exopolysaccharide Psl has been reported to increase tobramycin resistance in *P. aeruginosa* (Beaudoin et al., 2017).

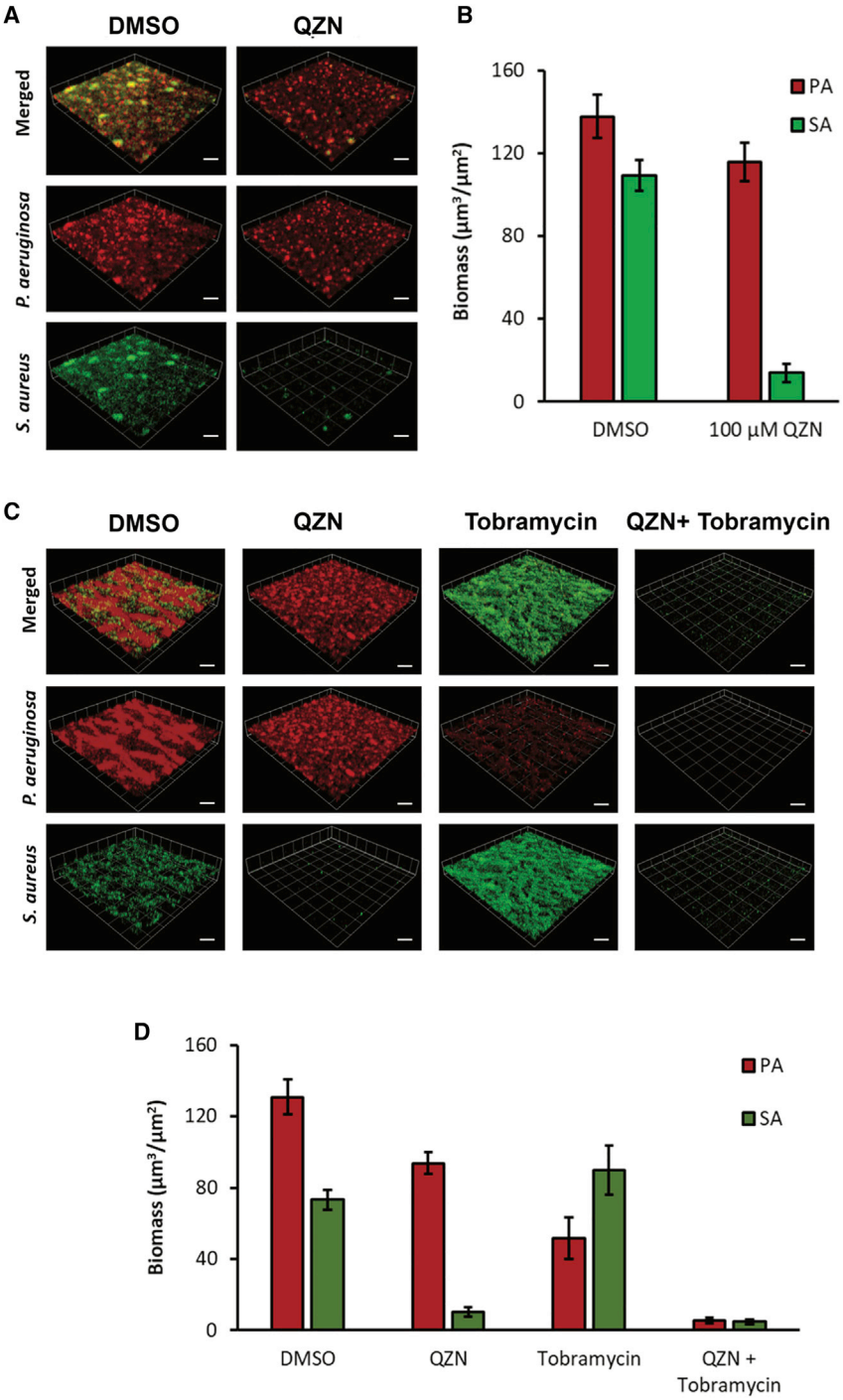

Figure 5. Impact of 3-C_3NH_2-7Cl-C9-QZN 34 and tobramycin on *P. aeruginosa* and *S. aureus* mixed biofilms

(A and B) 3-C_3NH_2-7Cl-C9-QZN **34** confers partial protection of *P. aeruginosa* (PA) in a mixed-species biofilm with *S. aureus* (SA). Biofilms were allowed to form on glass after sequential inoculation with GFP-labeled *S. aureus* SH1000 (green) and mCherry labeled *P. aeruginosa* PAO1 (red) in a 10:1 ratio in RPMI 1640 containing either DMSO (vehicle control) or QZN **34** (100 μM) and incubated for 48 h.

(C and D) Combined effect of 3-C_3NH_2-7Cl-C9-QZN **34** and tobramycin on a mixed-species biofilm. The biofilm was allowed to form on glass after sequential inoculation with GFP-labeled *S. aureus* SH1000 (green) and mCherry labeled *P. aeruginosa* PAO1 (red) in a 10:1 ratio in RPMI 1640 containing either DMSO (vehicle control) or QZN **34** (100 μM) and incubated for 48 h. For some experiments, tobramycin (100 μg/mL) was also added, and the biofilms were cultured for a further 4 h.

(A and C) show 3D confocal microscope images. (B and D) show biomass quantification of the mixed-species biofilms after treatment. Scale bars, 50 μm. Data are means from 3 independent experiments ± SD.

Following exposure of *P. aeruginosa* cell-free culture supernatants, *S. aureus* biofilms have been reported to become more sensitive to membrane-permeabilizing antibiotics and biocides (Orazi et al., 2019). This increase was associated with HQNO as well as the *P. aeruginosa* siderophores pyochelin and pyoverdine. HQNO biosynthesis depends on the PqsR-dependent expression of the *pqsABCDE* operon. Consequently, PqsR antagonists such as **34** inhibit the production of all AQs including HQNO as well as reducing siderophore production, since PQS also regulates the latter (Rampioni et al., 2016). Therefore, in mixed biofilms with *P. aeruginosa*, the susceptibility of *S. aureus* to the membrane-active **34** cannot be enhanced by HQNO, given that the QZN at 100 μM (over six times the IC_{50} for PqsR) is likely to have abolished HQNO production when provided following the initial seeding inoculation of both species in the biofilm assay. However, in mixed biofilms under these experimental conditions, **34** appears to be more active in reducing the *S. aureus* biofilm biomass than in the single-species biofilm (~7-fold compared with ~4-fold). Further work will therefore be required to determine whether the dual properties of **34** as both an inhibitor of HQNO production and a membrane-permeabilizing agent are counter-productive in a single antimicrobial agent in mixed biofilms at lower concentrations.

Alternative advantages of the 3-aminoalkyl-substituted QZNs as inhibitors of HQNO production by *P. aeruginosa* in biofilm co-culture is that this should avoid HQNO-mediated inhibition of the electron transport chain, which reduces the susceptibility of *S. aureus* to protein synthesis-inhibitory antibiotics, including the aminoglycosides, tetracyclines, and macrolides (Orazi et al., 2019).

When the mixed biofilm was treated with tobramycin (100 μg/mL), the aminoglycoside reduced the *P. aeruginosa* biomass by ~60%, but the *S. aureus* component of the biofilm was clearly protected by the presence of the Gram negative. Although the

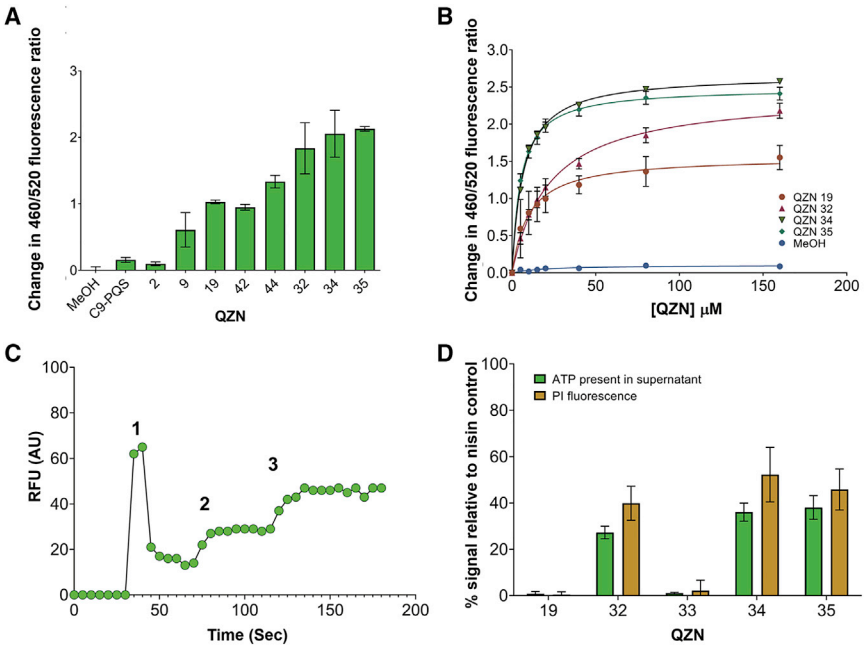

Figure 6. Affinity for and perturbation of the *S. aureus* cytoplasmic membrane by selected AQs and QZNs

(A) QZNs disturb the membrane dipole potential. Changes in dipole potential were determined using di-8-ANEPPS to measure the variation in the fluorescence ratio *R*(460/520) at a fixed concentration of 40 μM for each compound. Data are means from 3 independent experiments±SD

(B) Binding curves as a function of QZN concentration. The binding profiles for MeOH, **2**, **19**, **32**, **34**, and **35**. The data plotted are the mean values of three independent experiments; error bars represent standard deviations.

(C) Depolarization of transmembrane potential by **34**. (1) The cationic fluorescent dye DiSC3(5) was added to cells, followed (2) by 10 μM of test compound. Complete depolarization of the membrane potential was achieved by the addition of 5 μM valinomycin (3). Experiments were repeated on three independent occasions, with representative data shown.

(D) Membrane permeabilization. Cytoplasmic ATP release and PI fluorescence relative to nisin (0.6 μM; positive control) after treatment of *S. aureus* with 10 μM of compounds **19**, **32**, **33**, **34**, and **35**. The data plotted are the mean values of three independent experiments; error bars represent standard deviations.

mechanism involved has not yet been elucidated, in mixed *P. aeruginosa* and *Streptococcus* biofilms tobramycin treatment appears to enhance streptococcal biofilm formation as a consequence of a tobramycin-driven reduction in rhamnolipid production (Price et al., 2015). Furthermore, *S. aureus* may also be protected by *P. aeruginosa* biofilm matrix components including the exopolysaccharides Psl and Pel as well as eDNA (Ciofu and Tolker-Nielsen, 2019). In contrast, when the mixed biofilm was incubated with tobramycin after pre-treatment with **34**, most of the biofilm was killed, with less than 5% remaining. These data suggest that, in combination, tobramycin and the QZN are capable of eradicating both bacterial species in a mixed biofilm.

The bactericidal activity of the 3-aminoalkyl-substituted QZNs toward planktonic *S. aureus* suggested that these QZNs may target the cytoplasmic membrane. We therefore first investigated whether they possessed any affinity for the *S. aureus* cytoplasmic membrane by measuring dipole potential. This membrane potential originates via the molecular dipoles associated with carbonyl, oxygen-bonded phosphate moieties of phospholipids and is orientated toward water molecules at the membrane interface (O'Shea, 2005). Previously, we successfully used this technique to investigate the interactions of AHLs and tetramic and tetronic acids with both staphylococcal and eukaryotic membranes (Davis et al., 2010; Murray et al., 2014). For example, 3-tetradecanoyltetronic acid (C14-TOA), a membrane-active agent with a K_d of 4 μM, inhibited *agr*-dependent quorum sensing, reduced *S. aureus* colonization of human nasal epithelial cells, and showed efficacy in a staphylococcal experimental mouse infection model

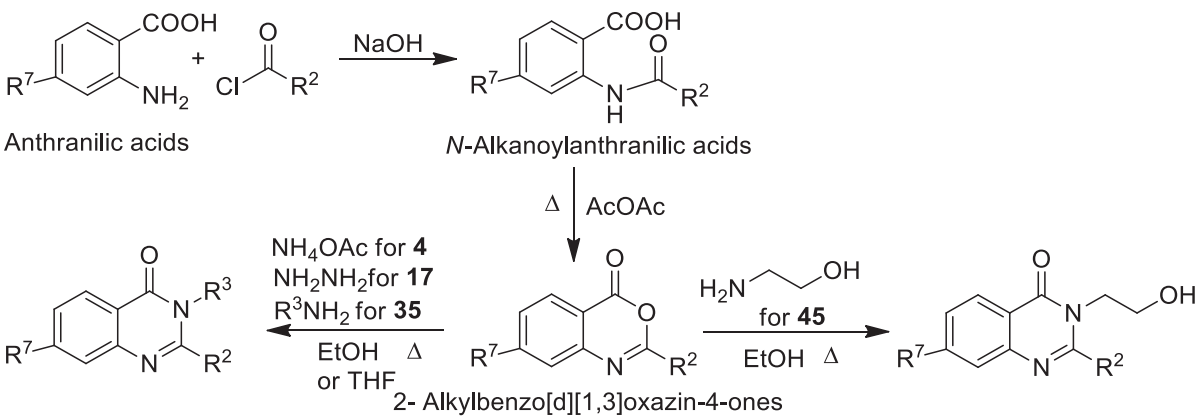

Scheme 1. Synthesis of 2-alkyl-4(3*H*)-quinazolinones (4, 17, 35, and 45)

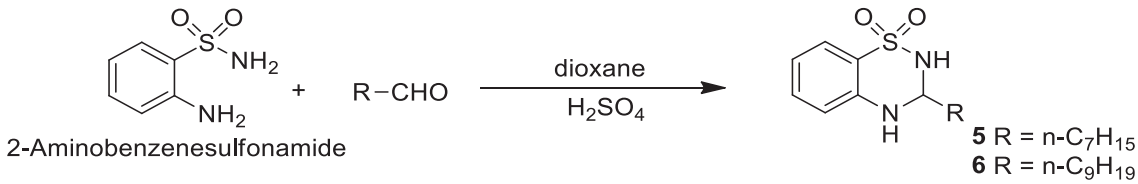

Scheme 2. Synthesis of 3-alkyl-3,4-dihydro-2H-benzo[e][1,2,4]thiadiazine 1,1-dioxide (5 and 6)

(Murray et al., 2014). Similar affinities for staphylococcal membranes were calculated from the binding curves for QZNs such as **34** and **35**, consistent with the presence of a specific saturable receptor. These data also indicated that anti-staphylococcal activity positively correlated with a low-value K_d, given the reduced membrane affinity of inactive QZNs such as compound **2**. Further investigation of the interactions of **32**, **34**, and **35** with the cytoplasmic membrane suggested that the Gram-positive bactericidal activity of these QZNs depends on a combination of membrane depolarization and pore formation leading to ATP release and cell death. Similar results have been reported for the clinically approved antibiotic daptomycin, although this lipopeptide antibiotic has also been shown to perturb fluid microdomains and, as a consequence, to interfere with membrane-bound cell wall and lipid biosynthesis (Müller et al., 2016). However, daptomycin lacks bactericidal activity against Gram-negative bacteria, and this appears to be independent of the outer-membrane permeability barrier (Miller et al., 2016). This may also be the case for the QZNs **32** and **34**, given that their antagonistic activity for PqsR requires their uptake into the *P. aeruginosa* cytoplasm.

Our findings of the efficacy of tobramycin in combination with the lead QZNs toward *P. aeruginosa* and *S. aureus* in mixed biofilms offers additional opportunities to exploit the QZN scaffold for the development of adjuvant drugs capable, in combination with antibiotics, of eradicating chronic wound and lung infections caused by these problematic pathogens.

SIGNIFICANCE

***Staphylococcus aureus* and *Pseudomonas aeruginosa* commonly cause biofilm-centered chronic infections in diverse body sites that are highly refractory to host immune defences and antibiotics. Their co-existence in polymicrobial biofilms within the same infection site often results in poor clinical outcomes. To survive in the same environmental niches, bacteria have evolved intricate regulatory networks that facilitate co-operative behavior through quorum sensing (QS) that facilitates evasion or suppression of other bacterial species as well as providing mutual benefit by forming antibiotic-tolerant biofilms. Given the global health threat posed by multi-antibiotic-resistant bacterial pathogens, novel antibacterial agents are required that have potent efficacy against biofilm-centered infections. In this context, QS systems have been viewed as attractive targets for drug molecules that inhibit biofilm formation and virulence and could be used alone or as adjuvants in combination with antibiotics. In *P. aeruginosa*, pseudomonas quinolone (PQS)-dependent QS can be attenuated via small-molecule antagonists targeting the transcriptional regulator PqsR. Here, we explored our library of quinazolinones (QZNs), which includes PqsR agonists and antagonists, for their activity against *S. aureus* alone, when co-cultured with *P. aeruginosa*, and in combination with tobramycin. We discovered that a subset of PqsR QZN antagonists not only perturbed *P. aeruginosa* biofilm development but also killed planktonic cells and effectively damaged *S. aureus* biofilms. Although *P. aeruginosa* protected *S. aureus* from tobramycin in mixed biofilms, the combination of the aminoglycoside antibiotic with a QZN eradicated mixed-species biofilms. The mechanism of action of the active QZNs toward *S. aureus* is shown to involve perturbation of the cytoplasmic membrane and dissipation of essential membrane electrical potentials. Our findings of the combined activity of tobramycin and the lead QZN toward *P. aeruginosa* and *S. aureus* in mixed biofilms offers additional opportunities to exploit the QZN scaffold for anti-infective drug development.**

STAR★METHODS

Detailed methods are provided in the online version of this paper and include the following:

- KEY RESOURCES TABLE
- RESOURCE AVAILABILITY
  - Lead contact
  - Materials availability
  - Data and code availability
- EXPERIMENTAL MODEL AND SUBJECT DETAILS
  - Bacterial strains and growth conditions
  - Mammalian cells
- METHOD DETAILS
  - Bacterial strain susceptibility testing
  - Bactericidal activity
  - Cytotoxicity
  - Chrome azurol S (CAS) iron chelation assay
  - Biofilm metabolic activity
  - Quantification of biofilm biomass
  - Biofilm viability assay
  - Bacterial membrane permeabilization assays
  - Membrane dipole potential
  - Dissipation of bacterial membrane potential
  - Chemical synthesis
  - 7-Chloro-2-n-nonylquinazolin-4(3*H*)-one (7Cl-C9-QZN) 4
  - *N*-Decanoyl-4-chloroanthranilic acid
  - 7-Chloro-2-n-nonyl-4*H*-benzo[d][1,3]oxazin-4-one
  - 7-Chloro-2-n-nonylquinazolin-4(3*H*)-one

- 3-Amino-2-methylquinazolin-4(3*H*)-one (3-NH_2-C1-QZN) 17
- 3-(4-Aminobutyl)-7-chloro-2-n-nonylquinazolin-4(3*H*)-one (3-C_4NH_2-7-Cl-C9-QZN) 35
- 7-Chloro-3-(2-hydroxyethyl)-2-n-nonylquinazolin-4(3*H*)-one (3-C_2OH-7Cl-C9-QZN) 45
- Synthesis of 3-alkyl-3,4-dihydro-2*H*-benzo[e][1,2,4] thiadiazine 1,1-dioxide (5 and 6)
- 3-n-Heptyl-3,4-dihydro-2*H*-benzo[e][1,2,4]thiadiazine 1,1-dioxide (C7-BTD) 5
- 3-n-Nonyl-3,4-dihydro-2*H*-benzo[e][1,2,4]thiadiazine 1,1-dioxide (C9-BTD) 6

- QUANTIFICATION AND STATISTICAL ANALYSIS

SUPPLEMENTAL INFORMATION

Supplemental information can be found online at https://doi.org/10.1016/j.chembiol.2022.02.007.

ACKNOWLEDGMENTS

We thank Alex Truman for QZN synthesis. This work was funded via a Medical Research Council UK program grant (MR/N010477/1) and a Wellcome Trust Senior Investigator grant (103884).

AUTHOR CONTRIBUTIONS

P.W. and S.R.C. conceived the project and supervised the work. P.W., E.M., and S.R.C. wrote the manuscript. E.M. and J.-F.D. designed and carried out the experimental work. All authors analyzed the data, contributed to and commented on the manuscript text, and approved its final version.

DECLARATION OF INTERESTS

The authors declare no competing interests.

Received: October 16, 2020
Revised: July 16, 2021
Accepted: February 15, 2022
Published: March 7, 2022

REFERENCES

Allesen-Holm, M., Barken, K.B., Yang, L., Klausen, M., Webb, J.S., Kjelleberg, S., Molin, S., Givskov, M., and Tolker-Nielsen, T. (2006). A characterization of DNA release in *Pseudomonas aeruginosa* cultures and biofilms. Mol. Microbiol. *59*, 1114–1128.

Barr, H.L., Halliday, N., Cámara, M., Barrett, D.A., Williams, P., Forrester, D.L., Simms, R., Smyth, A.R., Honeybourne, D., Whitehouse, J.L., et al. (2015). *Pseudomonas aeruginosa* quorum sensing molecules correlate with clinical status in cystic fibrosis. Eur. Respir. J. *46*, 1046–1054.

Barr, H.L., Halliday, N., Barrett, D.A., Williams, P., Forrester, D.L., Peckham, D., Williams, K., Smyth, A.R., Honeybourne, D., Whitehouse, J.L., et al. (2017). Diagnostic and prognostic significance of systemic alkyl quinolones for *P. aeruginosa* in cystic fibrosis: a longitudinal study. J. Cyst. Fibros. *16*, 230–238.

Beaudoin, T., Yau, Y., Stapleton, P.J., Gong, Y., Wang, P.W., Guttman, D.S., and Waters, V. (2017). *Staphylococcus aureus* interaction with *Pseudomonas aeruginosa* biofilm enhances tobramycin resistance. NPJ Biofilms Microbiomes *3*, 25.

Breeuwer, P., and Abee, T. (2000). Assessment of viability of microorganisms employing fluorescence techniques. Int. J. Food Microbiol. *55*, 193–200.

Castillo-Ramírez, S., Corander, J., Marttinen, P., Aldeljawi, M., Hanage, W.P., Westh, H., Boye, K., Gulay, Z., Bentley, S.D., Parkhill, J., et al. (2012). Phylogeographic variation in recombination rates within a global clone of methicillin-resistant *Staphylococcus aureus*. Genome Biol. *13*, R126.

Chiang, W.C., Nilsson, M., Jensen, P.Ø., Høiby, N., Nielsen, T.E., Givskov, M., and Tolker-Nielsen, T. (2013). Extracellular DNA shields against aminoglycosides in *Pseudomonas aeruginosa* biofilms. Antimicrob. Agents Chemother. *57*, 2352–2361.

Ciofu, O., and Tolker-Nielsen, T. (2019). Tolerance and resistance of *Pseudomonas aeruginosa* biofilms to antimicrobial agents-how *P. aeruginosa* can escape antibiotics. Front. Microbiol. *10*, 913.

Davis, B.M., Jensen, R., Williams, P., and O'Shea, P. (2010). The interaction of *N*-acylhomoserine lactone quorum sensing signaling molecules with biological membranes: implications for inter-kingdom signaling. PLoS One *5*, e13522.

DeLeon, S., Clinton, A., Fowler, H., Everett, J., Horswill, A.R., and Rumbaugh, K.P. (2014). Synergistic interactions of *Pseudomonas aeruginosa* and *Staphylococcus aureus* in an *in vitro* wound model. Infect. Immun. *82*, 4718–4728.

De Oliveira, D.M.P., Forde, B.M., Kidd, T.J., Harris, P.N.A., Schembri, M.A., Beatson, S.A., Paterson, D.L., and Walker, M.J. (2020). Antimicrobial resistance in ESKAPE pathogens. Clin. Microbiol. Rev. *33*, e00181-19.

Déziel, E., Gopalan, S., Tampakaki, A.P., Lépine, F., Padfield, K.E., Saucier, M., Xiao, G., and Rahme, L.G. (2005). The contribution of MvfR to *Pseudomonas aeruginosa* pathogenesis and quorum sensing circuitry regulation: multiple quorum sensing-regulated genes are modulated without affecting *lasRI, rhlRI* or the production of *N*-acyl-L-homoserine lactones. Mol. Microbiol. *55*, 998–1014.

Diggle, S.P., Matthijs, S., Wright, V.J., Fletcher, M.P., Chhabra, S.R., Lamont, I.L., Kong, X., Hider, R.C., Cornelis, P., Cámara, M., and Williams, P. (2007). The *Pseudomonas aeruginosa* 4-quinolone signal molecules HHQ and PQS play multifunctional roles in quorum sensing and iron entrapment. Chem. Biol. *14*, 87–96.

Dubern, J.F., Cigana, C., De Simone, M., Lazenby, J., Juhas, M., Schwager, S., Bianconi, I., Döring, G., Eberl, L., Williams, P., et al. (2015). Integrated whole-genome screening for *Pseudomonas aeruginosa* virulence genes using multiple disease models reveals that pathogenicity is host specific. Environ. Microbiol. *17*, 4379–4393.

Fazli, M., Bjarnsholt, T., Kirketerp-Møller, K., Jørgensen, B., Andersen, A.S., Krogfelt, K.A., Givskov, M., and Tolker-Nielsen, T. (2009). Nonrandom distribution of *Pseudomonas aeruginosa* and *Staphylococcus aureus* in chronic wounds. J. Clin. Microbiol. *47*, 4084–4089.

Fey, P.D., Endres, J.L., Yajjala, V.K., Widhelm, T.J., Boissy, R.J., Bose, J.L., and Bayles, K.W. (2013). A genetic resource for rapid and comprehensive phenotype screening of nonessential *Staphylococcus aureus* genes. mBio *4*, e00537-12.

Heeb, S., Fletcher, M.P., Chhabra, S.R., Diggle, S.P., Williams, P., and Camara, M. (2010). Quinolones: from antibiotics to autoinducers. FEMS Microbiol. Rev. *35*, 247–274.

Higgins, D.L., Chang, R., Debabov, D.V., Leung, J., Wu, T., Krause, K.M., Sandvik, E., Hubbard, J.M., Kaniga, K., Schmidt, D.E., Jr., et al. (2005). Telavancin, a multifunctional lipoglycopeptide, disrupts both cell wall synthesis and cell membrane integrity in methicillin-resistant *Staphylococcus aureus*. Antimicrob. Agents Chemother. *49*, 1127–1134.

Holden, M.T., Lindsay, J.A., Corton, C., Quail, M.A., Cockfield, J.D., Pathak, S., Batra, R., Parkhill, J., Bentley, S.D., and Edgeworth, J.D. (2010). Genome sequence of a recently emerged, highly transmissible, multi-antibiotic- and antiseptic-resistant variant of methicillin-resistant *Staphylococcus aureus*, sequence type 239 (TW). J. Bacteriol. *192*, 888–892. https://doi.org/10.1128/JB.01255-09.

Hooi, D.S., Bycroft, B.W., Chhabra, S.R., Williams, P., and Pritchard, D.I. (2004). Differential immune modulatory activity of Pseudomonas aeruginosa quorum-sensing signal molecules. Infect. Immun. *72*, 6463–6470.

Horsburgh, M.J., Aish, J.L., White, I.J., Shaw, L., Lithgow, J.K., and Foster, S.J. (2002). Sigma B modulates virulence determinant expression and stress resistance: characterization of a functional *rsbU* strain derived from *Staphylococcus aureus* 8325-4. J. Bacteriol. *184*, 5457–5467.

Hotterbeekx, A., Kumar-Singh, S., Goossens, H., and Maddocks, S. (2017). *In vivo* and *in vitro* interactions between *Pseudomonas aeruginosa* and *Staphylococcus* spp. Front. Cell. Infect. Microbiol. *7*, 1–13.

Ilangovan, A., Fletcher, M., Rampioni, G., Pustelny, C., Rumbaugh, K., Heeb, S., Cámara, M., Truman, A., Chhabra, S.R., Emsley, J., and Williams, P. (2013). Structural basis for native agonist and synthetic inhibitor recognition by the *Pseudomonas aeruginosa* quorum sensing regulator PqsR (MvfR). PLoS Pathog. *9*, e1003508.

Ji, G., Beavis, R.C., and Novick, R.P. (1995). Cell density control of staphylococcal virulence mediated by an octapeptide pheromone. Proc. Nat. Acad. Sci. U S A *92*, 12055–12059.

Kaufmann, G.F., Sartorio, R., Lee, S.H., Rogers, C.J., Meijler, M.M., Moss, J.A., Clapham, B., Brogan, A.P., Dickerson, T.J., and Janda, K.D. (2005). Revisiting quorum sensing: discovery of additional chemical and biological functions for 3-oxo-*N*-acylhomoserine lactones. Proc. Nat. Acad. Sci. U S A *102*, 309–314.

Kirchner, F.K. and Zalay, A.W. (1968). Certain alkyl and aryl substituted 3-amino-2, 3-dihydro-4(1h)quinazolinones. US patent 3375250.

Kirchner, F.K. and Zalay, A.W. (1974). 3-Amino-2,3-dihydro-4(1H)-quinazolinones. US patent 3843654.

Mahmoud, M.R., El-Bordany, E.A.A., Hassan, N.F., and El-Azm, F.S.M.A. (2007). New 2,3-disubstituted quinazolin-4(3H)-Ones from 2-undecyl-3,1-benzoxazin-4-one. J. Chem. Res. *9*, 541–544.

Miller, W.R., Bayer, A.S., and Arias, C.A. (2016). Mechanism of action and resistance to daptomycin in *Staphylococcus aureus* and Enterococci. Cold Spring Harb. Perspect. Med. *6*, a026997.

Müller, A., Wenzel, M., Strahl, H., Grein, F., Saaki, T.N.V., Kohl, B., Siersma, T., Bandow, J.E., Sahl, H.G., Schneider, T., and Hamoen, L.W. (2016). Daptomycin inhibits cell envelope synthesis by interfering with fluid membrane microdomains. Proc. Nat. Acad. Sci. U S A *113*, E7077–E7086.

Murray, E.J., Crowley, R.C., Truman, A., Clarke, S.R., Cottam, J.A., Jadhav, G.P., Steele, V.R., O'Shea, P., Lindholm, C., Cockayne, A., et al. (2014). Targeting *Staphylococcus aureus* quorum sensing with nonpeptidic small molecule inhibitors. J. Med. Chem. *57*, 2813–2819.

Novick, R.P., Ross, H.F., Projan, S.J., Kornblum, J., Kreiswirth, B., and Moghazeh, S. (1993). Synthesis of staphylococcal virulence factors is controlled by a regulatory RNA molecule. EMBO J. *12*, 3967–3975.

Nguyen, A.T., and Oglesby-Sherrouse, A.G. (2016). Interactions between *Pseudomonas aeruginosa* and *Staphylococcus aureus* during co-cultivations and polymicrobial infections. Appl. Microbiol. Biotechnol. *100*, 6141–6148.

Orazi, G., and O'Toole, G.A. (2019). "It takes a village": Mechanisms underlying antimicrobial recalcitrance of polymicrobial biofilms. J. Bacteriol *202*. e00530–19. https://doi.org/10.1128/JB.00530-19.

Orazi, G., Ruoff, K.L., and O'Toole, G.A. (2019). *Pseudomonas aeruginosa* increases the sensitivity of biofilm-grown *Staphylococcus aureus* to membrane-targeting antiseptics and antibiotics. mBio *10*, e01501–e01519.

O'Neill, E., Pozzi, C., Houston, P., Smyth, D., Humphreys, H., Robinson, D.A., and O'Gara, J.P. (2007). Association between methicillin susceptibility and biofilm regulation in *Staphylococcus aureus* isolates from device-related infections. J. Clin. Microbiol. *45*, 1379–1388.

O'Shea, P. (2005). Physical landscapes in biological membranes: physico-chemical terrains for spatio-temporal control of biomolecular interactions and behaviour. Philos. Trans. A Math. Phys. Eng. Sci. *363*, 575–588.

Ou, F., Mcgoverin, C., Swift, S., and Vanholsbeeck, F. (2016). Rapid evaluation of bacterial viability using the optrode – a near real time portable fluorimeter. Aust. Conf. Opt. Fiber Technol. AW3C.6. https://doi.org/10.1364/ACOFT.2016.

Peleg, A.Y., and Hooper, D.C. (2010). Hospital-acquired infections due to gram-negative bacteria. N. Engl. J. Med. *362*, 1804–1813.

Percival, S.L., Suleman, L., Vuotto, C., and Donelli, G. (2015). Healthcare-associated infections, medical devices and biofilms: risk, tolerance and control. J. Med. Microbiol. *64*, 323–334.

Popat, R., Crusz, S.A., Messina, M., Williams, P., West, S.A., and Diggle, S.P. (2012). Quorum-sensing and cheating in bacterial biofilms. Proc. Biol. Sci. *279*, 4765–4771.

Price, K.E., Naimie, A.A., Griffin, E.F., Bay, C., and O'Toole, G.A. (2015). Tobramycin-treated *Pseudomonas aeruginosa* PA14 Enhances *Streptococcus constellatus* 7155 biofilm formation in a cystic fibrosis model system. J. Bacteriol. *198*, 237–247.

Purcell, I. C. (2007). Bacterial autoinducer derived 4-quinolones as novel immune modulators. PhD Thesis, University of Nottingham. http://eprints.nottingham.ac.uk/10319/.

Qazi, S., Middleton, B., Muharram, S.H., Cockayne, A., Hill, P., O'Shea, P., Chhabra, S.R., Cámara, M., and Williams, P. (2006). *N*-Acylhomoserine lactones antagonize virulence gene expression and quorum sensing in *Staphylococcus aureus*. Infect. Immun. *74*, 910–919.

Rampioni, G., Pustelny, C., Fletcher, M.P., Wright, V.J., Bruce, M., Rumbaugh, K.P., Heeb, S., Cámara, M., and Williams, P. (2010). Transcriptomic analysis reveals a global alkyl-quinolone-independent regulatory role for PqsE in facilitating the environmental adaptation of *Pseudomonas aeruginosa* to plant and animal hosts. Environ. Microbiol. *12*, 1659–1673.

Rampioni, G., Leoni, L., and Williams, P. (2014). The art of antibacterial warfare: deception through interference with quorum sensing-mediated communication. Bioorg. Chem. *55*, 60–68.

Rampioni, G., Falcone, M., Heeb, S., Frangipani, E., Fletcher, M.P., Dubern, J.F., Visca, P., Leoni, L., Cámara, M., and Williams, P. (2016). Unravelling the genome-wide contributions of specific 2-alkyl-4-quinolones and PqsE to quorum sensing in *Pseudomonas aeruginosa*. PLoS Pathog. *12*, e1006029.

Schlechter, R.O., Jun, H., Bernach, M., Oso, S., Boyd, E., Munoz-Lintz, D.A., Dobson, R.C.J., Remus, D.M., and Remus-Emsermann, M.N.P. (2018). Chromatic Bacteria - a broad host-range plasmid and chromosomal insertion toolbox for fluorescent protein expression in bacteria. Front. Microbiol. *9*, 3052.

Schneider, C.A., Rasband, W.S., and Eliceiri, K.W. (2012). NIH Image to ImageJ: 25 years of image analysis. Nat. Methods *9*, 671–675.

Schwyn, B., and Neilands, J.B. (1987). Universal chemical assay for the detection and determination of siderophores. Anal. Biochem. *160*, 47–56.

Scott, J.R., Guenthner, P.C., Malone, L.M., and Fischetti, V.A. (1986). Conversion of an M- group A streptococcus to M+ by transfer of a plasmid containing an M6 gene. J. Exp. Med. *164*, 1641–1651.

Soukarieh, F., Williams, P., Stocks, M.J., and Cámara, M. (2018). *Pseudomonas aeruginosa* quorum sensing systems as drug discovery targets: current position and future perspectives. J. Med. Chem. *61*, 10385–10402.

Starkey, M., Lepine, F., Maura, D., Bandyopadhaya, A., Lesic, B., He, J., Kitao, T., Righi, V., Milot, S., Tzika, A., and Rahme, L. (2014). Identification of anti-virulence compounds that disrupt quorum-sensing regulated acute and persistent pathogenicity. PLoS Pathog. *10*, e1004321.

Tong, S.Y.C., Davis, J.S., Eichenberger, E., Holland, T.L., and Fowler, V.G., Jr. (2015). *Staphylococcus aureus* infections: epidemiology, pathophysiology, clinical manifestations, and management. Clin. Microbiol. Rev. *28*, 603–661.

Valenti-Weigand, P., Benkel, P., Rohde, M., and Chhatwal, G.S. (1996). Entry and intracellular survival of group B streptococci in J774 macrophages. Infect. Immun. *64*, 2467–2473.

Williams, P., and Camara, M. (2009). Quorum sensing and environmental adaptation in *Pseudomonas aeruginosa*: a tale of regulatory networks and multifunctional signal molecules. Curr. Opin. Microbiol. *12*, 182–191.

Williams, P. (2017). Strategies for inhibiting quorum sensing. Emerg. Top. Life Sci. *1*, 23–30.

Wilton, M., Charron-Mazenod, L., Moore, R., and Lewenza, S. (2015). Extracellular DNA acidifies biofilms and induces aminoglycoside

resistance in *Pseudomonas aeruginosa*. Antimicrob. Agents Chemother. *60*, 544–553.

Xiao, G., Déziel, E., He, J., Lépine, F., Lesic, B., Castonguay, M.H., Milot, S., Tampakaki, A.P., Stachel, S.E., and Rahme, L.G. (2006). MvfR, a key *Pseudomonas aeruginosa* pathogenicity LTTR-class regulatory protein, has dual ligands. Mol. Microbiol. *62*, 1689–1699.

Zapotoczna, M., Murray, E.J., Hogan, S., O'Gara, J.P., Chhabra, S.R., Chan, W.C., O'Neill, E., and Williams, P. (2017). 5-Hydroxyethyl-3-tetradecanoyltetramic acid represents a novel treatment for intravascular catheter infections due to *Staphylococcus aureus*. J. Antimicrob. Chemother. *72*, 744–753.

STAR★METHODS

KEY RESOURCES TABLE

REAGENT or RESOURCE	SOURCE	IDENTIFIER
Bacterial and virus strains		
S. aureus	(Novick et al., 1993)_	RN6390
S. aureus	(Horsburgh et al., 2002)	SH1000
S. aureus	(Fey et al., 2013)	USA300 JE2
S. aureus	(O'Neil et al., 2007)	BH1CC
S. aureus	(Holden, 2010)	TW20
S. aureus	(Castillo-Ramírez et al., 2012)	HU6
S. aureus	(Castillo-Ramírez et al., 2012)	HU24
S. aureus	(Castillo-Ramírez et al., 2012)	IU4
S. aureus	(Castillo-Ramírez et al., 2012)	IU9
S. aureus	(Castillo-Ramírez et al., 2012)	IU12
S. aureus	(Castillo-Ramírez et al., 2012)	DEU9
S. aureus	(Castillo-Ramírez et al., 2012)	DEU19
S. aureus	(Castillo-Ramírez et al., 2012)	DEU20
S. epidermidis	This laboratory	1455
E. coli	This laboratory	MG1655
P. aeruginosa	This Laboratory	PA01-N
S. pyogenes	(Scott et al., 1986)	JRS4
S. agalactiae	(Valenti-Weigand et al., 1996)	6313
C. difficile	Ed Kuijper Collection	8085054
C. difficile	Ed Kuijper Collection	8079089
B. subtilis	Bacillus Genetic Stock Centre	168
Chemicals, peptides, and recombinant proteins		
Müller–Hinton broth	Oxoid	Cat# CM0405
L-cysteine	Oxoid	Cat# CM1135
Brain Heart Infusion broth	Oxoid	Cat# LP0021
Yeast Extract	Sigma-Aldrich	Cat# C7352
C. difficile supplement	Oxoid	Cat# SR0096
Luria Broth	Oxoid	Cat# CM0996B
Defibrinated Rabbit Blood	TCS biosciences	Cat# RB052
Phosphate Buffered Saline	Sigma-Aldrich	Cat# P4417
Triton X-100	Sigma-Aldrich	Cat# T8787
Resazurin	Sigma-Aldrich	Cat# R7017
RPMI-1640 (Biofilm Studies)	Lonza	Cat# 12-918F
RPMI-1640 (Cell Culture)	Sigma-Aldrich	Cat# R7509
Penicillin Streptomycin mix	Sigma-Aldrich	Cat# P0781
Glutamine	Sigma-Aldrich	Cat# G7513
Fetal Bovine Serum	Sigma-Aldrich	Cat# F9665
Tobramycin	Sigma-Aldrich	Cat# T04014
Propidium Iodide	Sigma-Aldrich	Cat# P4170
Nisin	Sigma-Aldrich	Cat# N5764
di-8-ANEPPS	Thermo-Fisher	Cat# D3167
$Disc_3(5)$	Thermo-Fisher	Cat# D306
Valinomycin	Sigma-Aldrich	Cat# V0627

(*Continued on next page*)

Continued

REAGENT or RESOURCE	SOURCE	IDENTIFIER
Critical commercial assays		
LDH Cytotoxicity Assay Kit	Biochain	Cat# K6330400
Cell Titre-Glo kit	Promega	Cat# G7570
Experimental models: Cell lines		
Jurkat T cells	Stratech	PC-006-SIG
Recombinant DNA		
pMMR	(Popat et al., 2012)	Constitutive mCherry fluorescent reporter
pBK-miniTn7-egfp	(Popat et al., 2012)	Constitutive eGFP fluorescent reporter
Software and algorithms		
ImageJ	(Schneider et al., 2012)	https://imagej.nih.gov/ij/
Zen	Zeiss, Germany	www.zeiss.com
Graphpad Prism 8.0	GraphPad Software, USA	https://www.graphpad.com

RESOURCE AVAILABILITY

Lead contact

Requests for further information and requests for responding to material, resources and reagents should be directed to and will be fulfilled by the Lead Contact Paul Williams (paul.williams@nottingham.ac.uk).

Materials availability

There are restrictions to the availability of the QZN compounds and bacterial strains due to the lack of an external centralized repository for their distribution and our need to maintain the stock. We are glad to share the QZNs with reasonable compensation by requestor for its processing and shipping. Requests for QZNs and bacterial strains should be directed to the lead contact, Paul Williams (paul.williams@nottingham.ac.uk).

Data and code availability

The published article includes all biological data generated during this study. This study did not generate code. All data reported in this paper will be shared by the lead contact upon request.

EXPERIMENTAL MODEL AND SUBJECT DETAILS

Bacterial strains and growth conditions

The bacterial strains used in this study are listed in the key resources table. *S. aureus*, *S. epidermidis*, *P. aeruginosa*, *E. coli* and *B. subtilis* were grown in Müller–Hinton broth (MHB) *S. aureus* was also grown in MHB with 10% fetal bovine serum (FBS). *Strep. pyogenes* and *Strep. agalactiae* were grown statically in brain heart infusion (BHI) with 5% CO_2. *C. difficile* isolates were grown anaerobically in BHI supplemented with yeast extract, L-cysteine and *C. difficile* supplement. Bacteria were grown at 37°C.

Mammalian cells

Jurkat T cells were grown at 37°C in the presence of 5% CO_2. Growth medium was RPMI-1640 supplemented with a final concentration of 10% fetal bovine serum, 100 units penicillin, 0.1 mg/ml streptomycin and 2 mM glycine.

METHOD DETAILS

Bacterial strain susceptibility testing

MICs were determined by broth microdilution in the appropriate medium for bacterial growth.

Bactericidal activity

S. aureus, *S. epidermidis* and *P. aeruginosa* were grown overnight in Luria Broth, diluted 250-fold and grown to an OD_{600} 0.5. Cells were diluted to 1×10^6 per ml in challenge medium (LB plus QZN at 8 × MIC) or shock media (sterile water with or without 10 or 50 μM QZN and without or with 160 mOSm NaCl, KCl, or $CaCl_2$). Samples were removed at intervals and viable counts determined.

Cytotoxicity

Haemolytic activity was assessed by incubating defibrinated rabbit blood (TCS Biosciences) in phosphate buffered saline (PBS) for 60 min in the presence of test compound or Triton X-100 (positive control). Samples were pelleted and supernatants collected. % hemolytic activity was determined as A_{543} relative to the Triton X-100 treated control. Cytotoxicity for mammalian cells was measured using the BioChain® LDH cytotoxicity assay kit as per the manufacturer's instructions. Briefly, 2 x 10^4 Jurkat cells were incubated for 24 h in the presence of test compound or the lysis control agent. The A_{490} was measured and percentage cytotoxicity calculated relative to the positive lysis control.

Chrome azurol S (CAS) iron chelation assay

A 0.5 ml aliquot of phosphate buffered saline (PBS; pH 7.4) without (as a reference) or with the relevant compound (50 μM) was mixed with 0.5 ml of CAS assay solution prepared according to Schwyn and Neilands (1987). The sample (S) and reference (R) absorbances were determined at 630 nm after 15 min incubation at room temperature. The percentage of iron-chelating activity was calculated by subtracting the sample A_{630} from that of the reference A_{630} value. Siderophore units are defined as [A(r) – A(s)/A(r)] x 100.

Biofilm metabolic activity

The metabolic activity of staphylococcal biofilms was quantified using the redox sensitive dye resazurin as described previously (Zapotoczna et al., 2017). Briefly, cells were grown overnight in BHI, diluted to an OD_{600} of 0.1 and aliquoted into a 96 well plate. Staphylococci were incubated at 37°C for 3 h to allow for cell attachment. The growth medium was removed and the wells were washed with PBS before fresh BHI was added. Biofilms were challenged with QZN immediately after bacterial attachment or after 24 h of static growth and biofilm development at 37°C. After treatment with a QZN, biofilms were cultured for a further 24 h before Reaszurin fluorescence was quantified.

Quantification of biofilm biomass

Biofilms were cultivated on borosilicate glass coverslips in 6-well microplates (Corning). *P. aeruginosa* strain PAO1 (Washington subline) and *S. aureus* strain SH1000, were transformed respectively with plasmids pMMR or pMRE147 and pBK-miniTn7-egfp that constitutively express mCherry and a green fluorescent protein (GFP or mClover3 respectively) (Popat et al., 2012; Schlechter et al., 2018). The fluorescently tagged strains were grown at 37°C for 16 h in RPMI-1640 (Lonza, Slough, UK), diluted 1:100 (v/v) in fresh medium and allowed to grow until an OD_{600} of ~0.5 was reached. These cultures were diluted to OD_{600} 0.1 for *S. aureus* and 0.01 for *P. aeruginosa* in RPMI-1640 and inoculated into 6 well microplates containing UV sterilised borosilicate glass coverslips (22 × 22 mm, thickness no.1) (VWR, Lutterworth, UK). Bacterial cells were seeded onto the coverslip surface at 37°C under static conditions for 1 h before cultures incubated with shaking for 48 h for *S. aureus* or 24 h for *P. aeruginosa* to form mature biofilms. For the *S. aureus* biofilm killing assay, the medium was discarded after 48 h incubation and replaced by fresh RPMI-1640 containing 3-C_3NH_2-7Cl-C9-QZN **34** or tobramycin followed by a further 4h incubation. For *P. aeruginosa* biofilm inhibition assays, **34** was added to the inoculum and incubated for 24 h prior to tobramycin addition and a further 4 h of incubation. For the co-culture biofilm experiments, microplates were inoculated first with *S. aureus* and incubated statically for 1 h followed by *P. aeruginosa* in a 10:1 ratio. 3-C_3NH_2-7Cl-C9-QZN was added and the cultures incubated for 48 h at 37°C. Where required, tobramycin was then added to the 48 h-old co-cultures by a further 4h incubation. After incubation stained for extracellular DNA (eDNA) with propidium iodide (PI) or YOYO-1 (2 μM). Coverslips were directly examined under a confocal laser scanning microscope (Zeiss LSM2, Zeiss, Oberkochen, Germany) using eGFP and mCherry modes at an excitation wavelengths of 488 nm and 555 nm. Imaging was carried out using Zen 2011 imaging software (Zeiss, Oberkochen, Germany). A total of 5 Z-stacked images were collected per coverslip. Sampling was conducted at random from the central portion of each coverslip. Biomass was calculated using Image J (NIH, Bethesda, MD, USA) and Comstat 2.1. Software package (www.comstat.dk, Lyngby, Denmark). The percentage of live cells was determined as described by Ou et al. (2016).

Biofilm viability assay

Staphyloccocal cells were recovered from biofilms on coverslip surfaces by gentle sonication in an ultrasonic bath for 5 min at a frequency of 37 kHz. The removal of biofilm was confirmed using confocal microscopy. Bacterial cells were collected and OD_{600nm} adjusted to 0.1. Cell suspensions were serial diluted down to 10^{-8} and 10μl spotted onto LB agar plates. These were incubated at 30°C for 16 h followed by manual colony counting. Cell numbers were expressed as $\log_{10}$ CFU/ml.

Bacterial membrane permeabilization assays

Membrane permeabilization was evaluated by quantifying (a) ATP release (Higgins et al., 2005) and (b) the uptake of propidium iodide (PI). *S. aureus* strain USA300 JE2 was grown overnight in CYGP medium (Ji et al., 1995) washed with phosphate buffer (100 mM, pH 7), re-suspended to OD_{600} 0.1 and incubated at 37°C with a range of concentrations of each compound for 1 h. Nisin (0.6 μM) was used as a positive control. Cell-free supernatants were assayed for ATP content using

the Cell Titre-Glo kit (Promega). Staphylococcal cells were re-suspended in phosphate buffer (pH 7) containing PI (10 μg/ml), incubated in the dark at room temperature for 10 min. After washing, PI fluorescence (excitation: 575 nm; emission 630 nm) was quantified.

Membrane dipole potential

S. aureus membranes were prepared and labelled with the dipole potential fluorescent sensor 1-(3-sulfonatopropyl)-4-[β-2-(di-*n*-octylamino)-6-naphthylvinyl] pyridinium betaine (di-8-ANEPPS) (Invitrogen) and the K_d for each compound determined using the dual wavelength ratiometric method as described by Qazi et al. (2006).

Dissipation of bacterial membrane potential

Transmembrane potential was determined as described by Breeuwer and Abee (2000). Staphylococcal cells were suspended in potassium phosphate buffer (50 mM, pH 7) containing 5 μM of the cationic fluorescent dye $Disc_3(5)$ (Invitrogen). Fluorescence output was continually monitored over 200 s (excitation 650 nm, emission 680 nM). Once the fluorescent signal had reduced and stabilised the selected QZN was added to the appropriate final concentration. To confirm that the membrane potential was responsible for the uptake of the cationic dye, 5 μM valinomycin was added to completely depolarise the remaining membrane potential. As negative controls, the antibiotics novobiocin and chloramphenicol were also included at 10 μg/ml.

Chemical synthesis

QZNs (Table 1) were synthesized and characterized as described previously (Ilangovan et al., 2013) except for **4** (7-Cl-C9-QZN), **5** (C7-BTD), **6** (C9-BTD), **17** (3-NH_2-C1-QZN), **35** (3-C_4NH_2-7-Cl-C9-QZN) and **45** (3-C_2OH-7-Cl-C9-QZN). These were synthesised by the established literature procedures (Purcell, 2007; Kirchner and Zalay, 1968, 1974; Mahmoud et al., 2007), essentially in three steps as outlined in Scheme 1.

The acylation of appropriate anthranilic acids with acid chlorides gave *N*-alkanoylanthranilic acids which via dehydrative intramolecular cyclisation yielded 2-alkylbenzo[*d*] [1,3]oxazin-4-ones. The latter when aminated in refluxing ethanol (for **4**,**17**,**45**) or THF (for **35**) delivered the desired quinazolinones as crystalline solids after purification.

7-Chloro-2-n-nonylquinazolin-4(3*H*)-one (7Cl-C9-QZN) 4

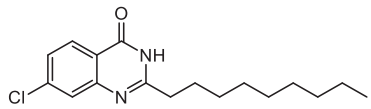

N-Decanoyl-4-chloroanthranilic acid

Decanoyl chloride (0.0275 mol) and a solution of sodium hydroxide, (0.025 mol) in water (10 mL) were simultaneously added dropwise over 15 min to a solution of 4-chloroanthranilic acid (0.025 mol) in sodium hydroxide (0.025 mol) dissolved in distilled water (10 mL) at 0-5°C. The resulting slurry was stirred at 0-5°C for 30 min followed by a further 30 min stirring at room temperature. The reaction mixture was then acidified to pH 1.0 with concentrated HCl (3.5 mL) and extracted with ethyl acetate (30 mL) which was washed with brine (10 mL), dried with magnesium sulphate and concentrated to dryness under reduced pressure. The resulting solid residue was stirred with petroleum ether bp 60-80°C (15 mL) for 1 h. The product was collected by filtration to give *N-decanoyl-4-chloroanthranilic acid* as a pale brown solid in 83% yield.

7-Chloro-2-n-nonyl-4*H*-benzo[d][1,3]oxazin-4-one

A mixture of *N*-decanoyl-4-chloroanthranilic acid (4.0 g) and acetic anhydride (25 mL) was stirred at reflux for 2 h. After cooling the solvent was removed under high vacuum to give the title compound.

7-Chloro-2-n-nonylquinazolin-4(3*H*)-one

A mixture of 7-chloro-2-*n*-nonyl-4*H*-benzo[d][1,3]-oxazin-4-one (0.3077 g, 1 mmol) and ammonium acetate (0.154 g, 2 mmol) was heated at 170°C for 2 h. The residue was cooled to room temperature and taken up in ethyl acetate (40 mL) and water (25 mL) which after 30 min of stirring the mixture was fully dissolved. The aqueous layer was removed and the organic layer was washed with saturated sodium bicarbonate, 1 M HCl, and brine. The organic layer was dried over magnesium sulphate and concentrated to dryness to give an off white solid which was purified using Flash chromatography (40% ethyl acetate in hexane) to deliver *7-chloro-2-n-nonyl-quinazolin-4(3H)-one* as a white solid (0.096 g, 31%).

^{1}H NMR ($CDCl_3$) δ 0.91 (3H, t, Me), 1.25-1.5 (12H, m, $(CH_2)_6$Me), 1.87 (2H, quintet, $CH_2(CH_2)_6$Me), 2.76 (2H, t, $CH_2(CH_2)_7$Me), 7.44 (1H, 6-H), 7.72 (1H, 8-H), 8.22 (1H, 5-H), 10.74 (1H, s, NH), ES-MS *m/z* 307.1572 $[M+H]^+$, $C_{17}H_{24}ClN_2O^+$ requires 307.1572).

3-Amino-2-methylquinazolin-4(3*H*)-one (3-NH_2-C1-QZN) 17

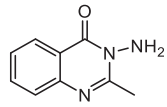

2-Methyl-*4H*-benzo[*d*][1,3]oxazin-4-one was prepared as a cream solid in quantitative yield from anthranilic acid (0.03 M) and acetic anhydride (25 ml) by the procedure described above under **5**. A solution of 2-Methyl-4*H*-benzo[d][1,3]oxazin-4-one (1 mmol) and hydrazine monohydrate (4 mmol) in ethanol (20 mL) was stirred at reflux overnight. The solvent was removed under reduced pressure to give the title compound as a cream solid 0.640 g (73% yield) which required no further purification.

^{1}H NMR ($CDCl_3$) δ 2.74 (3H, t, Me), 4.92 (2H, s, NH_2), 7.48 (1H, 8-H), 7.68 (1H, 6-H), 7.76 (1H, 7-H), 8.26 (1H, 5-H).

ES-MS *m/z* 176.0815 $[M+H]^+$, $C_9H_{10}N_3O^+$ requires 176.0818.

3-(4-Aminobutyl)-7-chloro-2-n-nonylquinazolin-4(3*H*)-one (3-C_4NH_2-7-Cl-C9-QZN) 35

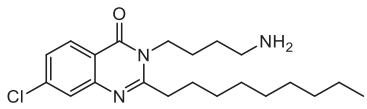

A solution of 7-chloro-2-n-nonyl-4*H*-benzo[*d*][1,3]oxazin-4-one (as described for **4**) (0.615 g, 2.0 mmol) and *N*-Boc-1,4-butanediamine (1.506 g, 8.0 mmol) in dry THF (20 mL) was stirred at reflux overnight. The solvent was removed under reduced pressure and the residue was dissolved in ethyl acetate (40 mL) and washed with saturated $NaHCO_3$ (2 x 15 mL), 1 M $KHSO_4$ (2 x 15 mL) and brine (15 mL). The organic layer was dried over magnesium sulphate and concentrated to dryness to give a pale brown oily solid which was purified using flash chromatography (10% ethyl acetate in hexane followed by 15% ethyl acetate in hexane) and trituration with diethyl ether/hexane to give *3-[3-(tert-butoxycarbonylamino)butyl]-7-chloro-2-n-nonyl-4(3H)-quinazolinone* as a white solid (0.303 g).

A solution of 3-[3-(*tert*-butoxycarbonylamino)butyl]-7-chloro-2-*n*-nonyl4(3*H*)-quinazolinone (0.130 g, 2.8 mmol) in DCM (7 mL) and trifluoroacetic acid (7 mL) was stirred overnight at room temperature. The solution was concentrated to dryness under reduced pressure with the aid of acetonitrile. The residue was dissolved in ethyl acetate (15 mL) and washed with saturated sodium bicarbonate (2 x 7.5 mL) and brine (7.5 mL). The organic layer was dried over magnesium sulphate and concentrated to dryness to give an oily solid which was purified by trituration with hexane and petroleum ether bp 40-60°C to give the title compound as a white solid (0.027 g, 13%).

^{1}H NMR ($CDCl_3$) δ 0.91 (3H, t, Me), 1.31-1.51 (12H, m, $(CH_2)_6$Me), 1.65 (2H, m, $CH_2CH_2CH_2CH_2NH_2$), 1.83 (4H, m, $CH_2CH_2CH_2CH_2NH_2$ and $CH_2(CH_2)_6$Me), 2.11 (2H, b, NH_2), 2.84 (4H, m, $CH_2(CH_2)_7$Me and $(CH_2)_3CH_2NH_2$), 4.11 (2H, t, $CH_2(CH_2)_3NH_2$), 7.39 (1H, 8-H), 7.65 (1H, 6-H), 8.18 (1H, 5-H).

ES-MS *m/z* 378.2312 $[M+H]^+$, $C_{21}H_{33}ClN_3O^+$ requires 378.2307.

7-Chloro-3-(2-hydroxyethyl)-2-n-nonylquinazolin-4(3*H*)-one (3-C_2OH-7Cl-C9-QZN) 45

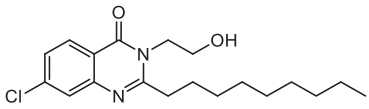

A solution of 7-chloro-2-n-nonyl-4*H*-benzo[d][1,3]oxazin-4-one (as described for **4**) (0.461 g, 1.5 mmol) and ethanolamine (0.367 g, 6 mmol) in ethanol (20 mL) was stirred at reflux overnight. The solvent was removed under reduced pressure and the residue was dissolved in ethyl acetate (30 mL) and washed with saturated $NaHCO_3$ (2 x 10 mL), 1 M KHSO4 (2 x 10 mL) and brine (10 mL). The organic layer was dried over magnesium sulphate and concentrated to dryness to give an off white solid which was purified using flash chromatography (10% ethyl acetate in hexane followed by 30% ethyl acetate in hexane and finally 70% ethyl acetate in hexane) to give the titled compound as a white solid (0.133 g, 25%).

^{1}H NMR ($CDCl_3$) δ 0.90 (3H, t, Me), 1.3-1.5 (12H, m, $(CH_2)_6$Me), 1.84 (2H, m, $CH_2(CH_2)_6$Me), 2.4 (1H, b, OH) 2.91 (2H, t, $CH_2(CH_2)_7$Me), 4.02 (2H, t, CH_2CH_2OH), 4.33 (2H, t, CH_2CH_2OH), 7.41 (1H, 8-H), 7.67 (1H, 6-H), 8.18 (1H, 5-H).

ES-MS *m/z* 351.1839 $[M+H]^+$, $C_{19}H_{28}ClN_2O_2^+$ requires 351.1834.

Synthesis of 3-alkyl-3,4-dihydro-2*H*-benzo[e][1,2,4]thiadiazine 1,1-dioxide (5 and 6)

The compounds **5** and **6** were synthesised by the acid catalysed cyclative condensation of 2-aminobenzenesulfonamide with an appropriate aldehyde in refluxing dioxane as outlined in Scheme 2.

3-n-Heptyl-3,4-dihydro-2*H*-benzo[e][1,2,4]thiadiazine 1,1-dioxide (C7-BTD) 5

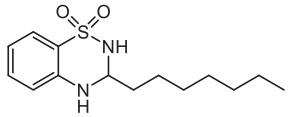

A solution of 2-aminobenzenesulfonamide (0.344 g, 2 mmol), octanal (0.282 g/0.343 ml, 2 mmol) and concentrated H_2SO_4 (4 drops) in dioxane (10 mL) was stirred at reflux for 3 h. The solvent was removed under reduced pressure and the orange oily solid was purified using flash chromatography (20% ethyl acetate in hexane) to give the title compound as an off white solid (0.159 g, 28%).

^{1}H NMR (DMSO-d_6) δ 0.88 (3H, t, Me), 1.29 (8H, m, *(CH$_2$)$_4$*Me), 1.46 (2H, m, *CH$_2$*(CH$_2$)$_4$Me), 1.74 (2H, m, *CH$_2$*(CH$_2$)$_5$Me), 4.63 (1H, m, (NH)$_2$*CH*CH$_2$(CH$_2$)$_6$Me), 6.69 (1H, t, 6-H), 6.81 (1H, d, 8-H), 6.97 (1H, s, 1-NH), 7.27 (1H, m, 7-H) 7.32 and 7.35 (1H, d, 3-NH), 7.45 (1H, d, 5H).

ES-MS *m/z* 283.1474 $[M+H]^+$, $C_{14}H_{23}N_2O_2S^+$ requires 283.1475.

3-n-Nonyl-3,4-dihydro-2*H*-benzo[e][1,2,4]thiadiazine 1,1-dioxide (C9-BTD) 6

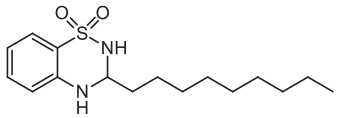

A solution of 2-aminobenzenesulfonamide (0.344 g, 2 mmol), decanal (0.343 g/0.415 ml, 2 mmol) and concentrated H_2SO_4 (4 drops) in dioxane (10 mL) was stirred at reflux for 3 h. The solvent was removed under reduced pressure and the brown oil was purified using flash chromatography (20% ethyl acetate in hexane) to give an impure cream solid. This was further purified by triturating with petroleum ether 60-80 (9 x 1.5 mL) to give the title compound as a white solid (0.078 g, 13%).

^{1}H NMR (DMSO-d_6) δ 0.87 (3H, t, Me), 1.27 (12H, m, *(CH$_2$)$_6$*Me), 1.45 (2H, m, *CH$_2$*(CH$_2$)$_6$Me), 1.74 (2H, m, *CH$_2$*(CH$_2$)$_7$Me), 4.64 (1H, m, (NH)$_2$*CH*CH$_2$(CH$_2$)$_6$Me), 6.69 (1H, t, 6-H), 6.81 (1H, d, 8-H), 6.99 (1H, s, 1NH), 7.27 (1H, m, 7-H) 7.33 and 7.36 (1H, d, 3NH), 7.43 (1H, d, 5H).

ES-MS *m/z* 311.1786 $[M+H]^+$, $C_{16}H_{27}N_2O_2S^+$ requires 311.1788.

QUANTIFICATION AND STATISTICAL ANALYSIS

Unless otherwise stated within the figure legend, each experiment was conducted on 3 independent occasions. Mean data is presented, error bars indicate the standard deviation. The biomass of each biofilm was assessed from 5 randomly selected sites and quantified using Image J software (Schneider et al., 2012).

Cell Chemical Biology, Volume *29*

Supplemental information

A *Pseudomonas aeruginosa* PQS quorum-sensing system inhibitor with anti-staphylococcal activity sensitizes polymicrobial biofilms to tobramycin

Ewan J. Murray, Jean-Frédéric Dubern, Weng C. Chan, Siri Ram Chhabra, and Paul Williams

Table S1. Minimum inhibitory concentrations of **32** (3-C_2NH_2-7Cl-C9-QZN)

Organism	**MIC µM** (µg/ml)
Staphylococcus aureus (MRSA and MSSA strains[§])	12.5 (4.4)
Staphylococcus epidermidis	6.25 (2.2)
Streptococcus pyogenes	6.25 (2.2)
Streptococcus. agalactiae	12.5 (4.4)
Clostridioides difficile ribotype-017	2.5 (0.9)
Clostridioides difficile ribotype-014	2.5 (0.9)
Bacillus subtilis 168	12.5 (4.4)
Escherichia coli MG1655	>100
Pseudomonas aeruginosa PAO1	>100

see [§]**Key Resources Table** for details of *S. aureus* strains tested

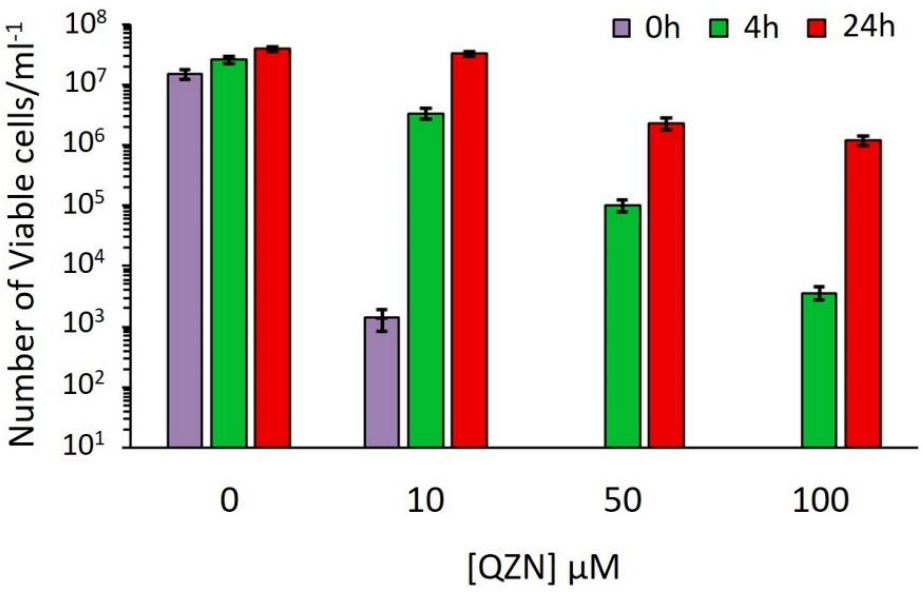

Figure S1. Related to Figure 3 and Star Methods (biofilm viability assay). Supporting evidence that 3-C_3NH_2-7Cl-C9-QZN (**34**) reduces the viability of *Staphylococcus aureus* biofilms. **34** (100 μM) was added to the culture at the time of inoculation, or after 4h or 24h of biofilm formation. The data presented are the mean viable counts (CFU) per ml from 5 biological replicates ±SD.

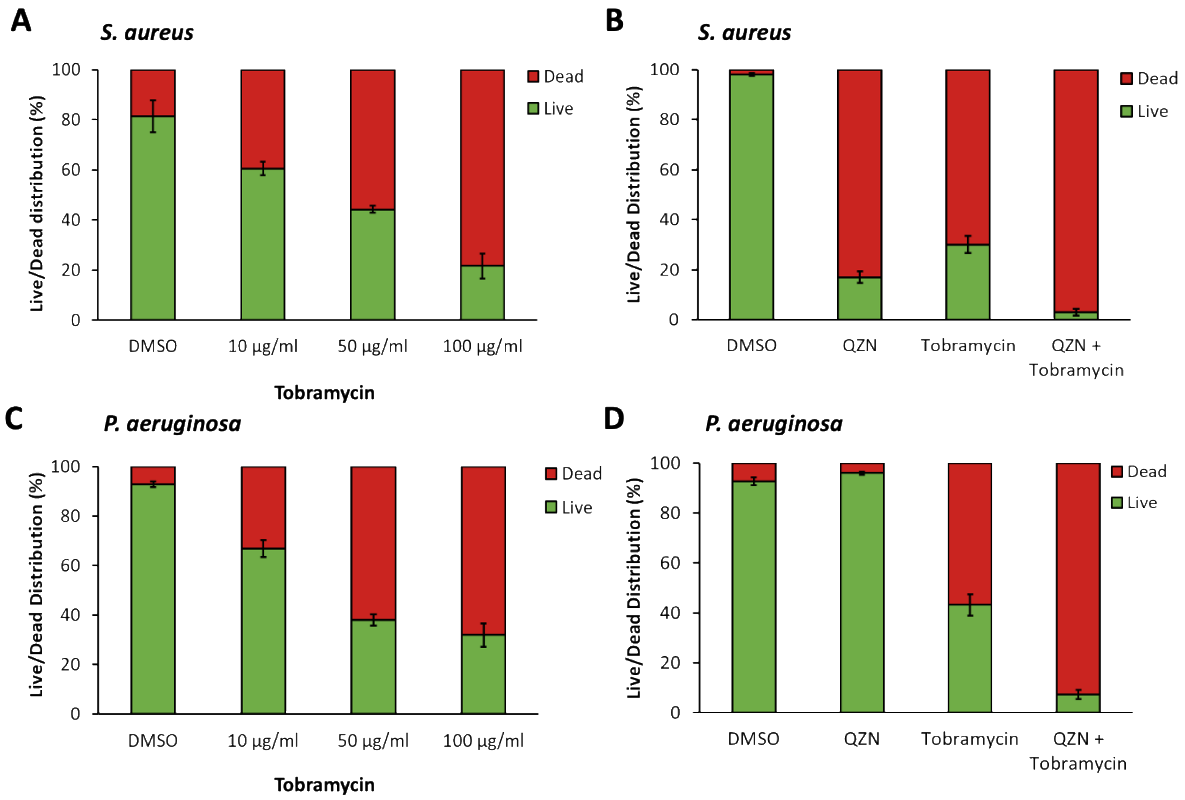

Figure S2 Related to Figure 5. Effect of tobramycin without (**A** and **C**) or with QZN **34** (**B** and **D**) on *S. aureus* SH1000 (**A** and **B**) or *P. aeruginosa* (**C** and **D**) biofilm viability in monocultures. *S. aureus* SH1000 and *P. aeruginosa* were fluorescently tagged with *gfp* and *mclover3* respectively. Biofilms were grown in the absence or presence of QZN (100 µM) prior to treatment for 4 h with tobramycin at 0, 10, 50 or 100 µg/ml. The relative distribution of live and dead cells was quantified using 3D confocal microscopy and image analysis after staining with propidium iodide.

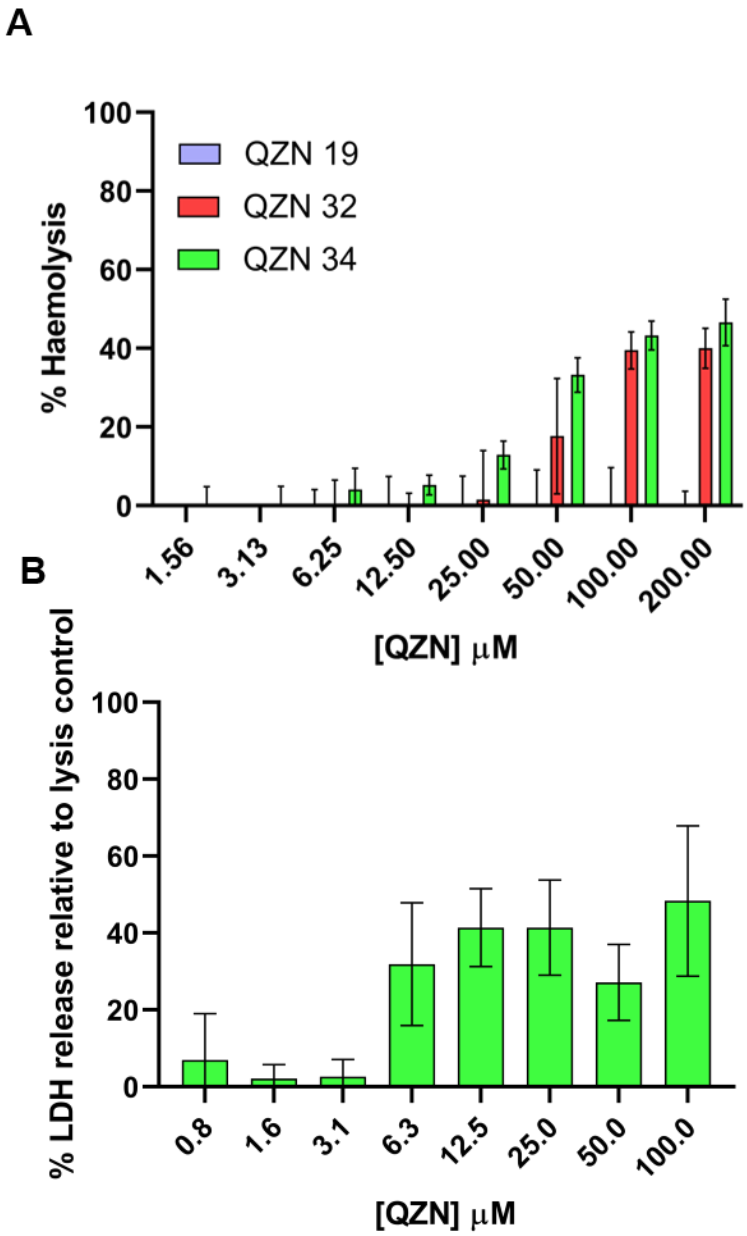

Figure S3. Related to Star Methods (mammalian cytotoxicity tests) for QZNs **19, 32 and 34.** (**A**) Haemolytic activity**.** QZNs were incubated with defibrinated rabbit red blood cells at a range of concentrations. Percentage haemolysis was calculated relative to a Triton X-100 control. The data plotted are the mean values of 3 independent experiments; error bars represent standard deviations. (**B**) Release of cytoplasmic LDH. 3-C_3NH_2-7Cl-C9-QZN **34** was incubated with Jurkat cells for 24 h at a range of concentrations. The data plotted are the mean values of 3 independent experiments; error bars represent standard deviations.

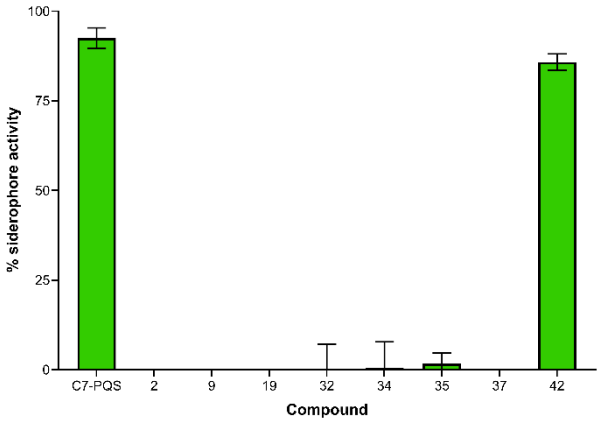

Figure S4. Related to Star Methods (Chrome Azurol S iron chelation assay). Determination of iron chelating properties of QZNs **2**, **9, 19**, **32**, **34**,**35, 37 and 42** 100 μM compared with PQS and relative to 10 μM deferoxamine.

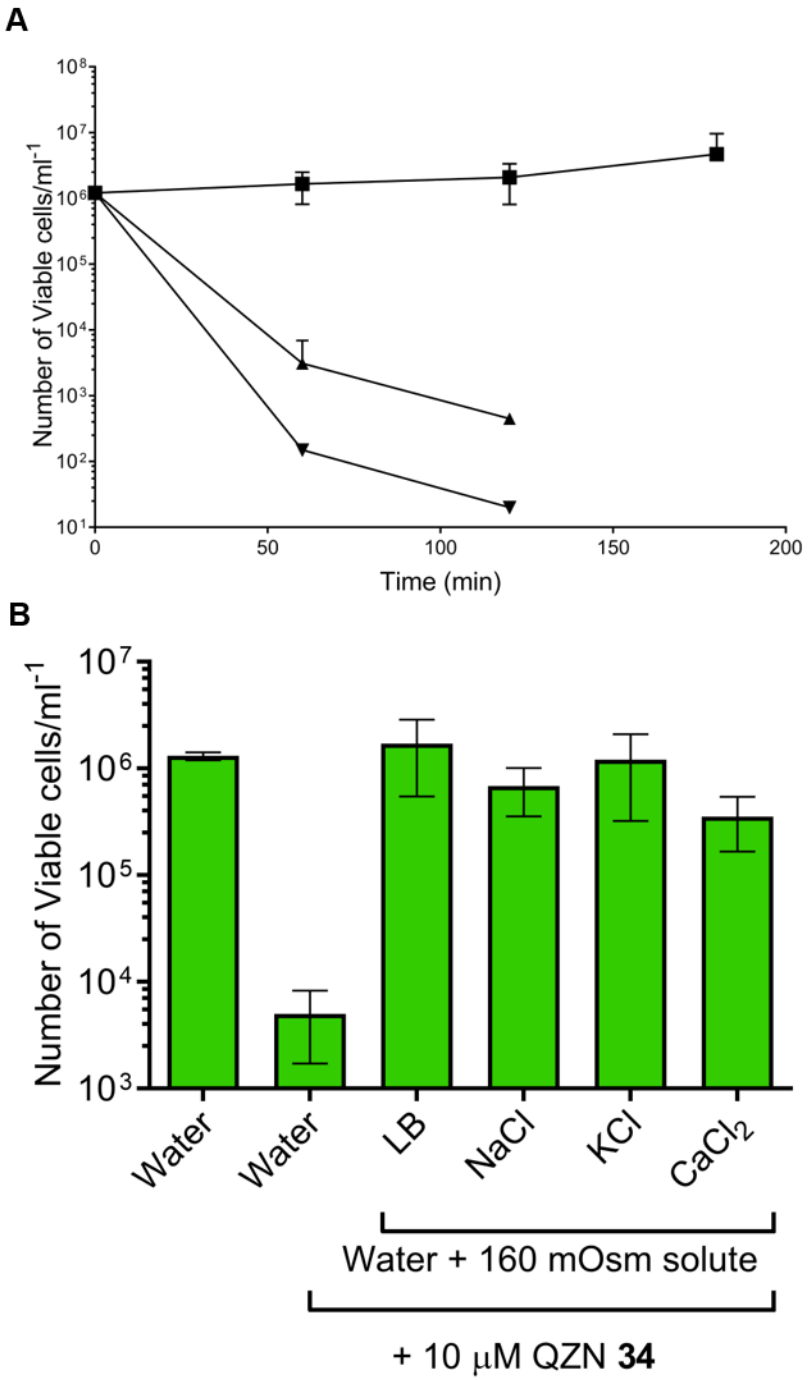

Figure S5. Related to Figure 2. Planktonic *S. aureus* were inoculated into sterile water (■), sterile water supplemented with 10 μM (▲) or sterile water supplemented with 50 μM (▼) compound **34**. The data presented are the mean viable counts (CFU) per ml from 3 independent experiments ±SD. (**B**) Planktonic *S. aureus* USA300 JE2 were inoculated into shock medium (10 μM compound **34**) in sterile water, LB or sterile water plus 160 mOsm of one of the following solutes: NaCl, KCl, $CaCl_2$. The data presented are the mean viable counts (CFU) per ml from 3 independent experiments ±SD.

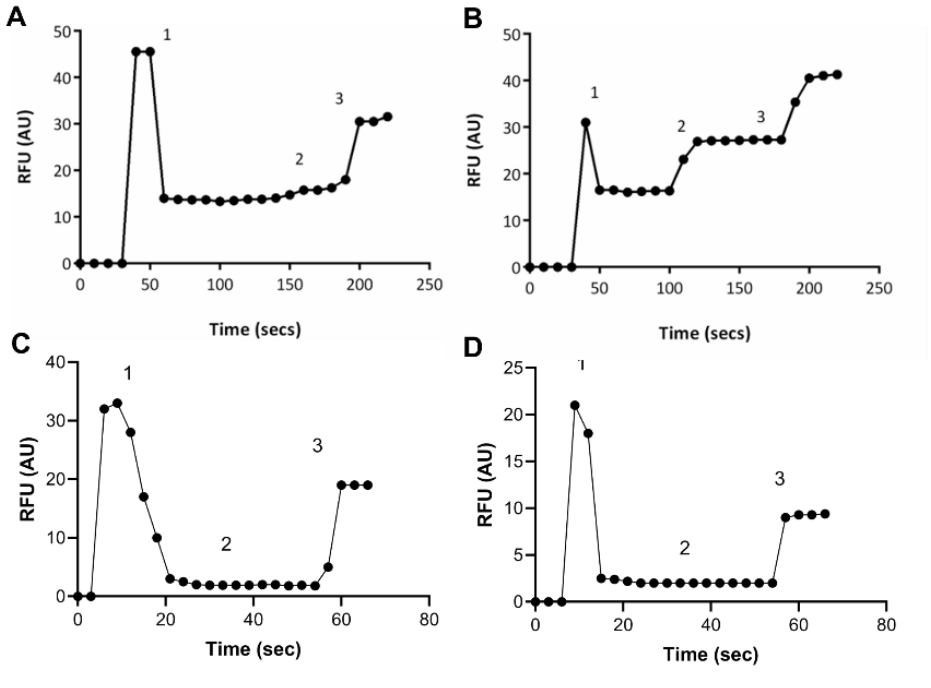

f

Figure S6. Related to Figure 6**.** Depolarisation of transmembrane potential in response to QZNs **19** (**A**) and **32** (**B**) or the antibiotics novobiocin (**C**) and chloramphenicol (**D**). (1) The cationic fluorescent dye DiSC3(5) was added to cells followed by (2) 10 μM (**19**: 3.2 μg/ml; **32**: 3.5 μg/ml) QZN or 10 μg/ml novobiocin or 10 μg/ml chloramphenicol. Complete depolarisation of the membrane potential was achieved by the addition of 5 μM valinomycin (3). Experiments were carried out on 3 independent occasions with representative data presented.